Visible and NIR hyperspectral imaging and chemometrics for prediction of microbial quality of beef *Longissimus dorsi m.* under simulated normal and abuse storage conditions

Achata Em, Oliveira M, Esquerre Ca, Tiwari Bk, O'Donnell Cp

PII: S0023-6438(20)30452-7

DOI: https://doi.org/10.1016/j.lwt.2020.109463

Reference: YFSTL 109463

To appear in: *LWT - Food Science and Technology*

Received Date: 30 December 2019

Revised Date: 13 April 2020

Accepted Date: 18 April 2020

Please cite this article as: Em, A., M, O., Ca, E., Bk, T., Cp, O'Donnell., Visible and NIR hyperspectral imaging and chemometrics for prediction of microbial quality of beef *Longissimus dorsi m.* under simulated normal and abuse storage conditions, *LWT - Food Science and Technology* (2020), doi: https://doi.org/10.1016/j.lwt.2020.109463.

CRediT authorship contribution statement

Eva Achata: Investigation, Data Curation, Formal analysis, Visualization, Writing - Original draft, **Marcia Oliveira:** Investigation, Data Curation **Carlos Esquerre:** Software, Writing - Review & Editing **Brijesh Tiwari:** Conceptualization, Methodology, Resources **Colm O'Donnell:** Conceptualization, Resources, Writing - Review & Editing, Supervision, Funding acquisition

Visible and NIR hyperspectral imaging and chemometrics for prediction of microbial quality of beef *Longissimus dorsi m.* under simulated normal and abuse storage conditions

Achata EM[1], Oliveira M[2], Esquerre CA[1], Tiwari BK[2], O'Donnell CP[1]

[1]School of Biosystems and Food Engineering, University College Dublin, Ireland

[2]Department of Food Chemistry & Technology, Teagasc Food Research Centre, Ashtown, Dublin 15, Ireland

Abstract

There is a need to develop a rapid technique to provide real time information on the microbial load of meat along the supply chain. Hyperspectral imaging (HSI) is a rapid, non-destructive technique well suited to food analysis applications. In this study, HSI in both the visible and near infrared spectral ranges, and chemometrics were studied for prediction of the bacterial growth on beef *Longissimus dorsi m.* (*LD*) under simulated normal (4 ºC) and abuse (10 ºC) storage conditions. Total viable count (TVC) prediction models were developed using partial least squares regression (PLS-R), spectral pre-treatments, band selection and data fusion methods. The best TVC prediction models developed for storage at 4 ($RMSE_p$ 0.58 log CFU/g, RPD_p 4.13, R^2_p 0.96), 10 ºC ($RMSE_p$ 0.97 log CFU/g, RPD_p 3.28, R^2_p 0.94) or at either 4 or 10 ºC ($RMSE_p$ 0.89 log CFU/g, RPD_p 2.27, R^2_p 0.86) were developed using high-level data fusion of both spectral regions. The use of appropriate spectral pre-treatments and band selection methods was key for robust model development. This study demonstrated the potential of HSI and chemometrics for real time monitoring to predict microbial growth on *LD* along the meat supply chain.

Key words: Hyperspectral imaging, chemometrics, TVC prediction, data fusion, meat.

1. Introduction

The *Longissimus dorsi m.* (*LD*) of beef is highly valued by consumers and is normally aged to increase tenderness, juiciness and flavour. Meat processors generally age *LD* for 28 days or longer to improve tenderness and flavour. However colour and microbial load are also affected which potentially impacts product safety and shelf life (Borch, Kant-Muermans, & Blixt, 1996; Vitale, Pérez-Juan, Lloret, Arnau, & Realini, 2014). The design and application of quality and safety assurance systems are based on thorough risk analysis and control of critical parameters through the entire life cycle of meat products including raw material selection and control during processing and distribution. The temperature profiles during transportation and at retail level are not within the direct control of meat processors and may exceed recommended temperatures. Lack of temperature control from retail to the time of preparation and consumption may also be an issue. In southern European countries 30% of refrigerated foods were reported to be stored above 10 ºC in retail cabinets and household refrigerators (Nychas, Skandamis, Tassou, & Koutsoumanis, 2008).

Current microbiological methods are not suitable for real time monitoring of microbial contamination of meat. The traditional plate count technique is the most commonly used method to monitor microbial load. However, it requires time consuming sample preparation and analysis. The total viable count (TVC) method is an important microbiology indicator for quality and safety evaluation of meat (Lytou, Panagou, & Nychas, 2016). The initial microbial load of meat after processing, storage temperature, pH and relative humidity are the main factors influencing microbial load throughout the supply chain. Enzyme-linked immune absorbent assay (ELISA), gene analysis-based methods such as polymerase chain reaction (PCR) and DNA sequencing are also employed for microbial contamination detection (Si et al., 2016) but are not suited to online analysis.

Visible (VIS) and near-infrared (NIR) spectroscopy are rapid non-destructive techniques widely used in environmental, pharmaceutical, fuel and food analysis applications. The VIS

and NIR spectral regions range from 380 - 740 nm and 700 - 2500 nm respectively. Spectroscopic sensors usually acquire spectra from a limited field of view which limits their applicability for rapid safety analysis of large volume batches or analysis of heterogeneous samples such as meat products (Millar, Moss, & Stevenson, 1996).

Hyperspectral imaging (HSI) is a rapid analytical tool for non-destructive measurement of food quality and safety. HSI integrates traditional imaging and spectroscopy to acquire both spatial and spectral information from samples. Each pixel in a hyperspectral image contains the spectrum of that specific position, i.e. the light-absorbing and/or scattering properties of the spatial region represented, which can be used to characterise the composition of that particular pixel (Gowen, O'Donnell, Cullen, Downey, & Frias, 2007; Kamruzzaman, Makino, & Oshita, 2016). HSI techniques can be employed at different points along meat distribution chains. HSI has been studied to predict microbial growth on fresh beef meat using the VIS range (Peng et al., 2011; Tao, Peng, Gomes, Chao, & Qin, 2015). However, no studies have been reported to date on the use of HSI in the NIR spectral range to predict microbial growth on fresh beef.

Chemometric methods are employed to develop prediction models from HSI data. Partial least squares regression (PLS-R) may be used to predict unknown concentrations and generate prediction maps to estimate spatial distributions of components in samples (Gowen, Burger, Esquerre, Downey, & O'Donnell, 2014). Spectral pre-treatments are used to correct for the effects of natural variability in the shape and size of samples, light scattering and differences in the effective path length in spectral data, which can present difficulties in the application of HSI for quality assessment (Esquerre, Gowen, Burger, Downey, & O'Donnell, 2012). Band selection methods have been demonstrated to improve the performance of regression models and to reduce the processing times required to evaluate HSI data by selecting the most informative bands. The variable importance projection method (VIP), the selectivity ratio method (SR) and the ensemble Monte Carlo variable selection method

(EMCVS) have been demonstrated to be reliable band selection methods for HSI data (Achata, Inguglia, Esquerre, Tiwari, & O'Donnell, 2019; Farrés, Platikanov, Tsakovski, & Tauler, 2015).

Data fusion combines information from different sources to produce a more reliable and accurate model or information. Three levels of data fusion may be employed i) low level (data-level) fusion, where data from all sources are properly transformed and concatenated for model development, ii) mid-level (feature-level) fusion, where variable selection or feature extraction is applied to each data source before the extracted features are combined; iii) and high-level (decision-level) fusion where a model is constructed for each data source separately and their predictions combined thereafter (Liu & Brown, 2004). Data fusion has been studied to detect volatile basic nitrogen (TVB-N) content in chicken meat using a colorimetric sensor and a VIS system (Khulal, Zhao, Hu, & Chen, 2017).

The objective of this study was to investigate the potential of HSI and chemometrics for the prediction of the microbial quality of beef under simulated normal (4 ºC) and abuse (10 ºC) storage conditions.

2. Materials and methods

2.1. Sample preparation

LD samples (n = 104) from 9 cattle (denoted S1 to S9) of ca. 25 mm thickness were obtained from local supermarkets and a meat processing facility. The samples were placed in sealed food containers and randomly assigned for storage at either 4 ºC (n = 53) for 360 hours or at 10 ºC (n = 51) for 168 hours. Three randomly selected samples (from 3 cattle) were removed from storage and scanned using a visible short wave near infrared (VIS-SWNIR) and an NIR HSI systems. The TVC of samples was measured after scanning using the ISO 48833-1:2013 methodology (ISO, 2013). Briefly 25 g of each sample was suspended in 225 ml of buffered peptone water (BPW, Oxoid, Hampshire, England) and aseptically homogenized in a

stomacher (Star-Blender LB 400, VWR) for 2 min. Further decimal dilutions were made with maximum recovery diluent (MRD, HyServe, Germany). Three replicates were assessed per sample at each sampling time. Reported populations represent the mean of three values.

2.2. Hyperspectral images

Hyperspectral images of the *LD* samples were obtained using a VIS-SWNIR HSI system (400 – 1000 nm) and an NIR HSI system (880 – 1720 nm) (DV Optics, Padova, Italy). Calibration of both HSI systems was performed as outlined by Achata, Esquerre, O'Donnell, and Gowen (2015). The acquired hypercubes were saved in ENVI formatted files and imported into MATLAB (The MathWorks Inc., Natick, MA, USA) for further spatial and spectral data pre-processing and chemometric analysis, using in-house developed functions and scripts.

2.2.1. VIS-SWNIR HSI spatial and spectral pre-processing

The noise present at both ends of the spectra was removed by trimming the spectral range to 445 - 970 nm. The background was removed using a mask created using the ratio between bands 80 (840 nm) and 20 (540 nm) and removing pixels with a ratio value > 1.5. To improve the signal-to-noise ratio (SNR) and reduce processing times and data storage required, 2×2 binning was performed on the obtained hypercubes of 1000 x 580 pixel image with 106 spectral bands, resulting in hypercubes of 500 x 290 pixel image with 106 spectral bands. The binned 3-dimensional hypercubes were unfolded into matrices of pixel spectra (14500 pixel x 106 spectral bands) to facilitate algorithm development. The mean reflectance (R) spectra of each masked sample was calculated and smoothed using the Savitzky - Golay (SG) 5 points second order polynomial method prior to chemometric analysis (Savitzky & Golay, 1964).

2.2.2. NIR-HSI spatial and spectral pre-processing

The noise present at both ends of the spectra was removed by trimming the spectral range to 957 - 1664 nm. Dead pixels and spikes were removed by replacing the affected values with the mean values of adjacent bands in the same spectrum. The background was removed using a mask which was created with the ratio between bands 90 (1580 nm) and 20 (1090 nm), removing pixels with a ratio value > 0.65. Images were segmented using the pixel ratio between bands 37 (1209 nm) and 43 (1251 nm) to remove fat and connective tissue (ratio value > 0.7). The 3-dimensional hypercubes (500 x 320 pixel image with 102 bands) were unfolded into matrices of pixel spectra (160000 pixel x 102 bands). The mean reflectance spectra of each segmented sample was calculated and smoothed using the Savitzky - Golay (SG) 5 points second order polynomial method prior to chemometric analysis.

2.3. Chemometric analysis

2.3.1. PCA

PCA (not reported) was carried out to investigate the relationships between storage temperature over time and spectral data, and to identify potential outliers using the Hoteling T^2 statistic. A sample was considered as an outlier if the T^2 value was > $T^2crit = A \times F_{(0.05,A,n-A)} \times (n-1)/(n-A)$, where A is the number of significant components, n is the number of spectra in the dataset and $F_{(0.05,A,n-A)}$ is the F statistic (with $\alpha = 0.05$, A and $n - A$ degrees of freedom).

2.3.2. PLS-R

PLS regression (Wold, Sjöström, & Eriksson, 2001) models were developed to predict TVC of samples using HSI data, spectral pre-treatments, band selection and data fusion methods.

Spectral data sets were split into calibration and validation sets to develop and validate the prediction models. Smoothed mean spectral data from 4 randomly selected samples (S1, S2, S4 and S6 (n=69)) was used for calibration and samples (S3 and S5) were used to validate the models (n=35). Predictions models were evaluated using the:

i) Smoothed mean spectral data of samples stored at 4 ºC (n = 53)

ii) Smoothed mean spectral data of samples stored at 10 ºC (n = 51)

iii) Smoothed mean spectral data of samples stored at either 4 or 10 ºC (n = 104).

The number of latent variables (LV) were selected by analysis of the root mean square error of ten-fold cross-validation ($RMSE_{CV}$) presented in Eq. (1) and roughness of the regression vector.

$$RMSE = \sqrt{\frac{\sum_{i=1}^{n}(y_i - \hat{y}_i)^2}{n}} \quad (1)$$

y_i and $\hat{y}_i$ are the measured and predicted values of the microbial counts respectively.

2.3.3. Spectral pre-treatments

Standard normal variate (SNV), median scaled (MS), Savitzky-Golay 7 points second order polynomial first derivative (FD), Savitzky-Golay 7 points second order polynomial second derivative (SD), Savitzky-Golay 11 points fourth order polynomial third derivative (TD), linear detrending second-order polynomial (LD), asymmetric least squares (AsLs) (Barnes, Dhanoa, & Lister, 1989; Boelens, Eilers, & Hankemeier, 2005; Engel et al., 2013; Savitzky & Golay, 1964) and all combinations of any two spectral pre-treatments were applied. The Savitzky-Golay derivative (FD, SD or TD) window length and polynomial order were selected by preliminary tests on 10 randomly selected spectra.

2.3.4. Band selection

The VIP (Eriksson, Hermens, Johansson, Verhaar, & Wold, 1995; Wold et al., 2001), SR (Rajalahti et al., 2009) and the EMCVS (Esquerre, Gowen, O'Gorman, Downey, & O'Donnell, 2017) band selection methods were evaluated and compared with and without spectral pre-treatments.

The performance of the regression models was assessed using the root mean square error (RMSE), the ratio of standard deviation of the reference data of the calibration set and the RMSE (RPD) and the coefficient of determination (R^2) for calibration (C), cross-validation (CV) and prediction (P) sets (Eq. 2-4). The best model was selected based on the number of latent variables, selected wavebands and the geometric mean of the RPD values from calibration, cross-validation, and prediction sets. Prediction models developed for complex matrices can be classified as excellent (RPD > 4.1), very good (RPD 3.5 – 4.0), good (RPD 3.0 – 3.4), fair (RPD 2.5 – 2.9) and poor (RPD 2.0 – 2.4) (Williams, 2014).

$$RPD = \frac{\mathrm{S_{ycal}}}{\mathrm{SEP}} \quad (2)$$

$$SEP = \sqrt{\frac{\sum_{i=1}^{n}(y_i - \hat{y}_i - \mathrm{bias})^2}{n-1}} \quad (3)$$

$$R^2 = \left(\frac{\sum_{i=1}^{n}(y_i \hat{y}_i) - n\bar{y}\,\bar{\hat{y}}}{\sqrt{\sum_{i=1}^{n} y_i^2 - n\bar{y}^2}\sqrt{\sum_{i=1}^{n} \hat{y}_i^2 - n\bar{\hat{y}}^2}} \right)^2 \quad (4)$$

Where the *bias* is the average difference between reference value and predicted value (Eq. 5).

$$bias = \frac{\sum_{i=1}^{n}(y_i - \hat{y}_i)}{n} \quad (5)$$

2.3.5. Data fusion

Prediction models for TVC of samples were developed for low level (LL), medium level (ML) and high-level (HL) data fusion of VIS-SWNIR and NIR HSI data. For the LL data fusion, the spectral data of both systems was concatenated before model development. For the ML data fusion, the selected spectral bands (obtained by the band selection method that achieved the best performance for each system) were combined. When the variance of the

pre-treated VIS-SWNIR and NIR HSI data was different, each data block was scaled to unit variance. The calibration, validation and prediction sets were scaled using the inverse of the standard deviation of the calibration set (Forshed, Idborg, & Jacobsson, 2007). For the HL data fusion, prediction models were developed by averaging the predictions of the best performing models identified for each system.

3. Results and discussion

3.1. TVC of samples

The TVC of *LD* samples during storage at 4 ºC and 10 ºC are presented in Table 1. TVC values increased from 3.4 to 14.1 log CFU/g over 360 h storage at 4 ºC and increased from 3.4 to 13.1 log CFU/g over 168 h storage at 10 ºC. Initial TVC values (day 0) varied according to the origin of the *LD* samples. *LD* S1 to S6 samples were purchased from local supermarkets and had initial TVC values > 6 log CFU/g. However, *LD* samples purchased directly from the meat processing facility (S7 to S9) had lower initial TVC values. *LD* S9 (non aged) samples had the lowest TVC values (3.4 log CFU/g), while samples from the *LD* S7 and S8 which were both aged for 28 days had TVC values of ca. 5.3 log CFU/g.

Previous studies reported that *LD* samples with TVC values < 7 log CFU/g are acceptable, and samples with values > 7 log CFU/g are spoiled (Tao et al., 2015). Moreover, the presence of slime and discolouration has been reported for meat samples with TVC values > 7 log CFU/g (Bell & Garout, 1994).

3.2. Spectral characteristics of *LD* samples

PCA analysis revealed the presence of one outlier in the VIS-SWNIR spectra of the *LD* samples stored at 4 ºC, which was removed from the dataset. No outliers were identified in the NIR spectra. Figs. 1 and 2 show the spectral variations between samples during storage at 4 and 10 ºC respectively. The SD + AsLs pre-treated log (1/R) NIR spectra were used for

TVC prediction at 4 ºC, whereas the SD+MS pre-treated reflectance VIS-SWNIR spectra were selected for TVC prediction at 10 ºC. Spectral shifts are more apparent during storage due to changes in physical characteristics, chemical composition and microbial activity. Spoiled samples exhibited broader absorption bands compared to unspoiled samples.

Absorbance peaks observed at 1076 and 1342 nm in Fig. 1 may be related to the C-H stretching of the first and second overtone regions respectively, and the peak at 1580 nm may be related to the 1st overtone of O-H stretching (glucose) (Osborne, Fearn, & Hindle, 1993). The selected bands highlighted in Fig.1 provide complementary information on the samples and are related to the 2nd overtone of O-H stretching (978 nm) of water and the 1st overtone of N-H stretching (1496 nm) of protein. Similar spectral bands were observed by Barbin, ElMasry, Sun, Allen, and Morsy (2013) for pork samples. The observed differences between spoiled and fresh meat may relate to the presence of protein, free amino acids, amines or nitrogen bearing substances and their interactions with water. Such observations are consistent with the proteolytic changes which occur during microbial spoilage (Atanassova, Veleva, & Stoyanchev, 2018).

Fig. 2 shows the characteristic peaks of the of oxymyoglobin ($MbFe^{II}O_2$) at 545 and 580 nm (Achata et al., 2019; Alamprese, Casale, Sinelli, Lanteri, & Casiraghi, 2013; Millar et al., 1996). These bands are prominent at the start of storage and increase in intensity after 24 h storage at 10 ºC (TVC < 7.3 log CFU/g). The intensity of these bands decreases after 48 h corresponding to TVC values > 7.5 log CFU/g. These changes may correspond to a decrease in the concentration of red pigments due to microbial growth during storage. The prominent peak at 765 nm may be related to the 3rd overtone C-H stretching. The selected bands highlighted in Fig. 2 provide complementary information on the samples and may be related to the 3rd overtone of C-H stretching (750 - 780 nm) (Osborne et al., 1993).

3.3. TVC prediction models

SD, SNV and the combination of SD+LD, and SNV+SD were identified as the best performing spectral pre-treatments after evaluating 50 combinations for each band selection method (Appendix 1). Models developed using the variable selection approach were compared with the best models developed using the full spectral range for both the VIS-SWNIR and NIR HSI spectral regions.

The best performing PLS-R model developed to predict TVC during storage at 4 ºC (Table 2) was developed using the NIR-HSI data and EMCVS of the SD+AsLs pre-treated log(1/R) spectra (17 selected bands, LV 7, $RMSE_P$ 0.81 log CFU/g, RPD_P 3.09, R^2_P 0.95). Lower coefficients of determination for the prediction of pork meat TVC were obtained by Barbin et al. (2013). Fig. 3a shows the predicted versus measured TVC values for *LD* samples stored at 4 ºC obtained with the SD+AsLs pre-treated log(1/R) spectra. HL data fusion improved the performance of the prediction models ($RMSE_P$ 0.58 log CFU/g, RPD_P 4.13, R^2_P 0.96) compared to those obtained with LL data fusion, ML data fusion and the best models selected for the VIS-SWNIR and NIR HSI spectral data (Table 5).

The best performing PLS-R model developed to predict TVC during storage at 10 ºC (Table 3) was developed using the VIS-SWNIR - HSI data and EMCVS of the SD+MS pre-treated reflectance spectra (46 selected bands, LV 6, $RMSE_P$ 0.96 log CFU/g, RPD_P 3.32, R^2_P 0.94). Fig.3b. shows the predicted versus measured TVC values for *LD* samples stored at 10 ºC obtained with the SD+MS pre-treated reflectance spectra. The use of derivative pre-treatments of VIS-SWNIR spectra has been reported to accentuate the differences in myoglobin spectra (Millar et al., 1996) by removing baseline offsets and decreasing scattering effects (Esquerre et al., 2012) as observed in Fig. 2. LL and HL data fusion yielded good prediction models, comparable to those obtained with the VIS-SWNIR data and better than the models developed using ML data fusion (Table 5).

The best performing PLS-R models developed to predict TVC for samples stored at either 4 or 10 ºC (Table 4) were developed using the VIS-SWNIR data and EMCVS of the SNV+SD pre-treated reflectance spectra (8 selected bands, LV 4, RMSEP 0.95 log CFU/g, RPD_P 2.10, R^2_P 0.85). Improved data fusion PLS-R models were developed using the LL and HL data fusion showed in Table 5 ($RMSE_P$ 0.87 log CFU/g, RPD_P 2.27, R^2_P 0.88, and $RMSE_P$ 0.89 log CFU/g, RPD_P 2.27, R^2_P 0.86 respectively). Fig. 3c shows the predicted versus measured TVC values of *LD* stored at either 4 or 10 ºC obtained using HL data fusion of both spectral regions.

Selected TVC prediction maps built using the best prediction model developed for storage at 10 ºC (SD+MS on the reflectance VIS-SWNIR spectra) are shown in Fig. 4.

Good and excellent TVC prediction models were obtained for beef *LD* samples stored at 4 ºC for both the NIR spectral range and HL data fusion of the VIS-SWNIR and NIR spectral regions respectively based on the RPD prediction model performance classifications reported by Williams (2014) for complex matrices. Good TVC prediction models were also obtained for samples stored at 10 ºC using the VIS-SWNIR spectral range and HL data fusion of both spectral regions. However poor TVC prediction models were obtained for samples stored at either 4 ºC or 10 ºC using the VIS-SWNIR spectral range and HL data fusion of both spectral regions. In all cases EMCVS outperformed the other band selection methods evaluated. Combinations of SD, SNV and LD spectral pre-treatments also improved regression model development. Data fusion approaches improved prediction model performance in all cases. This is in agreement with the study reported by (Li, Chen, Zhao, and Wu (2015)) who reported that superior regression models can be obtained using data fusion and appropriate band selection methods.

4. Conclusions

Excellent ($RMSE_p$ 0.58 log CFU/g, RPD_p 4.13, R^2_p 0.96) and good ($RMSE_p$ 0.97 log CFU/g, RPD_p 3.28, R^2_p 0.94) TVC prediction models were developed for beef *LD* samples stored at 4 ºC and 10 ºC respectively, using the HL data fusion of the two spectral regions. Prediction models were successfully developed using spectral pre-treatments, the full spectral range, selected bands and data fusion of both VIS-SWNIR and NIR spectral regions to predict the TVC of *LD* samples with low prediction errors.

The application of SD and SNV spectral pre-treatments improved the performance of the developed models using both spectral ranges and on selected bands. EMCVS improved the performance of the TVC prediction models developed compared with the full spectral range and outperformed VIP and SR methods. Data fusion approaches improved prediction model performance in all cases, HL data fusion yielded the best TVC prediction models ($RMSE_p$ 0.89 log CFU/g, RPD_p 2.27, R^2_p 0.86) for beef samples stored at both 4 ºC and 10 ºC. Appropriate band selection was key for robust model development. This study demonstrated the potential of HSI and chemometrics as a rapid analytical tool for monitoring meat microbial quality along the supply chain.

Acknowledgement

The authors acknowledge funding for this project from FIRM (13/FM/508) as administered by the Irish Department of Agriculture, Food & the Marine.

References

Achata, E. M., Esquerre, C. A., O'Donnell, C. P., & Gowen, A. A. (2015). A study on the application of near infrared hyperspectral chemical imaging for monitoring moisture content and water activity in low moisture systems. *Molecules, 20*(2), 2611.

Achata, E. M., Inguglia, E. S., Esquerre, C. A., Tiwari, B. K., & O'Donnell, C. P. (2019). Evaluation of Vis-NIR hyperspectral imaging as a process analytical tool to classify brined pork samples and predict brining salt concentration. *Journal of Food Engineering, 246*, 134-140. doi: 10.1016/j.jfoodeng.2018.10.022

Alamprese, C., Casale, M., Sinelli, N., Lanteri, S., & Casiraghi, E. (2013). Detection of minced beef adulteration with turkey meat by UV–vis, NIR and MIR spectroscopy. *LWT - Food Science and Technology, 53*(1), 225-232. doi: https://doi.org/10.1016/j.lwt.2013.01.027

Atanassova, S., Veleva, P., & Stoyanchev, T. (2018). Chapter 10 - Near-Infrared Spectral Informative Indicators for Meat and Dairy Products, Bacterial Contamination, and Freshness Evaluation. In A. M. Holban & A. M. Grumezescu (Eds.), *Microbial Contamination and Food Degradation* (pp. 315-340): Academic Press.

Barbin, D. F., ElMasry, G., Sun, D.-W., Allen, P., & Morsy, N. (2013). Non-destructive assessment of microbial contamination in porcine meat using NIR hyperspectral imaging. *Innovative Food Science & Emerging Technologies, 17*, 180-191. doi: https://doi.org/10.1016/j.ifset.2012.11.001

Barnes, R. J., Dhanoa, M. S., & Lister, S. J. (1989). Standard Normal Variate Transformation and De-Trending of Near-Infrared Diffuse Reflectance Spectra. *Applied Spectroscopy, 43*(5), 772-777. doi: 10.1366/0003702894202201

Bell, R. G., & Garout, A. M. (1994). The effective product life of vacuum-packaged beef imported into Saudi Arabia by sea, as assessed by chemical, microbiological and organoleptic criteria. *Meat Science, 36*(3), 381-396. doi: https://doi.org/10.1016/0309-1740(94)90134-1

Boelens, H. F. M., Eilers, P. H. C., & Hankemeier, T. (2005). Sign Constraints Improve the Detection of Differences between Complex Spectral Data Sets: LC−IR As an Example. *Analytical Chemistry, 77*(24), 7998-8007. doi: 10.1021/ac051370e

Borch, E., Kant-Muermans, M.-L., & Blixt, Y. (1996). Bacterial spoilage of meat and cured meat products. *International Journal of Food Microbiology, 33*(1), 103-120. doi: https://doi.org/10.1016/0168-1605(96)01135-X

Engel, J., Gerretzen, J., Szymańska, E., Jansen, J. J., Downey, G., Blanchet, L., & Buydens, L. M. C. (2013). Breaking with trends in pre-processing? *TrAC Trends in Analytical Chemistry, 50*, 96-106. doi: https://doi.org/10.1016/j.trac.2013.04.015

Eriksson, L., Hermens, J. L. M., Johansson, E., Verhaar, H. J. M., & Wold, S. (1995). Multivariate analysis of aquatic toxicity data with PLS. *Aquatic Sciences, 57*(3), 217-241. doi: 10.1007/BF00877428

Esquerre, C., Gowen, A. A., Burger, J., Downey, G., & O'Donnell, C. P. (2012). Suppressing sample morphology effects in near infrared spectral imaging using chemometric data pre-treatments. [Article]. *Chemometrics and Intelligent Laboratory Systems, 117*, 129-137. doi: 10.1016/j.chemolab.2012.02.006

Esquerre, C. A., Gowen, A. A., O'Gorman, A., Downey, G., & O'Donnell, C. P. (2017). Evaluation of ensemble Monte Carlo variable selection for identification of metabolite markers on NMR data. *Analytica Chimica Acta, 964*, 45-54. doi: https://doi.org/10.1016/j.aca.2017.01.027

Farrés, M., Platikanov, S., Tsakovski, S., & Tauler, R. (2015). Comparison of the variable importance in projection (VIP) and of the selectivity ratio (SR) methods for variable

selection and interpretation. *Journal of Chemometrics, 29*(10), 528-536. doi: 10.1002/cem.2736

Forshed, J., Idborg, H., & Jacobsson, S. P. (2007). Evaluation of different techniques for data fusion of LC/MS and 1H-NMR. *Chemometrics and Intelligent Laboratory Systems, 85*(1), 102-109. doi: https://doi.org/10.1016/j.chemolab.2006.05.002

Gowen, A., Burger, J., Esquerre, C., Downey, G., & O'Donnell, C. (2014). Near infrared hyperspectral image regression: On the use of prediction maps as a tool for detecting model overfitting. [Article]. *Journal of Near Infrared Spectroscopy, 22*(4), 261-270. doi: 10.1255/jnirs.1114

Gowen, A. A., O'Donnell, C. P., Cullen, P. J., Downey, G., & Frias, J. M. (2007). Hyperspectral imaging - an emerging process analytical tool for food quality and safety control. *Trends in Food Science and Technology, 18*(12), 590-598. doi: 10.1016/j.tifs.2007.06.001

ISO. (2013). International standard ISO 4833-2:2013: Microbiology of the food chain - Horizontal method for the enumeration of microorganisms - Part 1: Colony count at 30 °C by the pour plate technique.

Kamruzzaman, M., Makino, Y., & Oshita, S. (2016). Hyperspectral imaging for real-time monitoring of water holding capacity in red meat. *LWT - Food Science and Technology, 66*, 685-691. doi: https://doi.org/10.1016/j.lwt.2015.11.021

Khulal, U., Zhao, J., Hu, W., & Chen, Q. (2017). Intelligent evaluation of total volatile basic nitrogen (TVB-N) content in chicken meat by an improved multiple level data fusion model. *Sensors and Actuators B: Chemical, 238*, 337-345. doi: https://doi.org/10.1016/j.snb.2016.07.074

Li, H., Chen, Q., Zhao, J., & Wu, M. (2015). Nondestructive detection of total volatile basic nitrogen (TVB-N) content in pork meat by integrating hyperspectral imaging and colorimetric sensor combined with a nonlinear data fusion. *LWT - Food Science and Technology, 63*(1), 268-274. doi: https://doi.org/10.1016/j.lwt.2015.03.052

Liu, Y., & Brown, S. D. (2004). Wavelet multiscale regression from the perspective of data fusion: new conceptual approaches. [journal article]. *Analytical and Bioanalytical Chemistry, 380*(3), 445-452. doi: 10.1007/s00216-004-2776-x

Lytou, A., Panagou, E. Z., & Nychas, G.-J. E. (2016). Development of a predictive model for the growth kinetics of aerobic microbial population on pomegranate marinated chicken breast fillets under isothermal and dynamic temperature conditions. *Food Microbiology, 55*, 25-31. doi: https://doi.org/10.1016/j.fm.2015.11.009

Millar, S. J., Moss, B. W., & Stevenson, M. H. (1996). Some observations on the absorption spectra of various myoglobin derivatives found in meat. *Meat Science, 42*(3), 277-288. doi: https://doi.org/10.1016/0309-1740(94)00045-X

Nychas, G.-J. E., Skandamis, P. N., Tassou, C. C., & Koutsoumanis, K. P. (2008). Meat spoilage during distribution. *Meat Science, 78*(1), 77-89. doi: https://doi.org/10.1016/j.meatsci.2007.06.020

Osborne, B. G., Fearn, T., & Hindle, P. T. (1993). *Practical NIR spectroscopy with applications in food and beverage analysis.* Essex, England: Longman Scientific & Technical ; Wiley.

Peng, Y., Zhang, J., Wang, W., Li, Y., Wu, J., Huang, H., . . . Jiang, W. (2011). Potential prediction of the microbial spoilage of beef using spatially resolved hyperspectral scattering profiles. *Journal of Food Engineering, 102*(2), 163-169. doi: https://doi.org/10.1016/j.jfoodeng.2010.08.014

Rajalahti, T., Arneberg, R., Kroksveen, A. C., Berle, M., Myhr, K.-M., & Kvalheim, O. M. (2009). Discriminating Variable Test and Selectivity Ratio Plot: Quantitative Tools for Interpretation and Variable (Biomarker) Selection in Complex Spectral or

421 Chromatographic Profiles. *Analytical Chemistry, 81*(7), 2581-2590. doi:
422 10.1021/ac802514y
423 Savitzky, A., & Golay, M. J. E. (1964). Smoothing and Differentiation of Data by Simplified
424 Least Squares Procedures. *Analytical Chemistry, 36*(8), 1627-1639. doi:
425 10.1021/ac60214a047
426 Si, Y., Grazon, C., Clavier, G., Rieger, J., Audibert, J.-F., Sclavi, B., & Méallet-Renault, R.
427 (2016). Rapid and accurate detection of Escherichia coli growth by fluorescent pH-
428 sensitive organic nanoparticles for high-throughput screening applications. *Biosensors*
429 *and Bioelectronics, 75*, 320-327. doi: https://doi.org/10.1016/j.bios.2015.08.028
430 Tao, F., Peng, Y., Gomes, C. L., Chao, K., & Qin, J. (2015). A comparative study for
431 improving prediction of total viable count in beef based on hyperspectral scattering
432 characteristics. *Journal of Food Engineering, 162*, 38-47. doi:
433 https://doi.org/10.1016/j.jfoodeng.2015.04.008
434 Vitale, M., Pérez-Juan, M., Lloret, E., Arnau, J., & Realini, C. E. (2014). Effect of aging time
435 in vacuum on tenderness, and color and lipid stability of beef from mature cows
436 during display in high oxygen atmosphere package. *Meat Science, 96*(1), 270-277.
437 doi: https://doi.org/10.1016/j.meatsci.2013.07.027
438 Williams, P. (2014). The RPD Statistic: A Tutorial Note. *NIR news, 25*(1), 22-26. doi:
439 10.1255/nirn.1419
440 Wold, S., Sjöström, M., & Eriksson, L. (2001). PLS-regression: a basic tool of chemometrics.
441 *Chemometrics and Intelligent Laboratory Systems, 58*(2), 109-130. doi:
442 https://doi.org/10.1016/S0169-7439(01)00155-1

443

Appendix 1. Performance of the TVC PLS-R models developed using VIS-SWNIR (445 - 970 nm) data from beef *LD* samples stored at 4 ºC. PLS full spectral range on reflectance (R) and logarithmic transformed (log(1/R)) spectral data is compared with spectral pre-treatments (SNV, SD, SD+LD, SNV+SD) and band selection methods (VIP, SR and EMCVS).

Chemometric method	Spectral	Pre-treatment	# Bands	# LV	Calibration RMSEc	Calibration RPDc	Calibration R^2c	Cross validation RMSEcv	Cross validation RPDcv	Cross validation R^2cv	Prediction RMSEp	Prediction RPDp	Prediction R^2p
PLS	R	None	106	7	0.91	2.73	0.87	1.48	1.69	0.68	1.72	1.20	0.72
		SNV	106	7	0.84	2.97	0.89	1.20	2.08	0.78	1.62	1.37	0.78
		SD	100	8	0.61	4.09	0.94	1.08	2.30	0.82	2.16	1.21	0.71
		SD+LD	100	8	0.61	4.10	0.94	1.09	2.30	0.82	2.05	1.23	0.71
		SNV+SD	100	6	0.79	3.15	0.90	1.34	1.86	0.74	1.35	1.61	0.81
	Log(1/R)	None	106	3	1.27	1.96	0.74	1.59	1.56	0.60	1.79	1.20	0.58
		SNV	106	5	0.89	2.79	0.87	1.16	2.16	0.78	1.45	1.45	0.75
		SD	100	6	0.63	3.94	0.94	1.06	2.37	0.82	1.93	1.22	0.67
		SD+LD	100	6	0.64	3.87	0.93	1.05	2.39	0.82	1.83	1.25	0.67
		SNV+SD	100	4	0.82	3.06	0.89	1.24	2.04	0.76	1.45	1.44	0.75
VIP	R	None	7	2	1.27	1.97	0.74	1.41	1.77	0.68	1.79	1.33	0.66
		SNV	27	6	0.97	2.58	0.85	1.20	2.07	0.77	1.80	1.25	0.75
		SD	28	7	0.94	2.65	0.86	1.38	1.81	0.70	1.78	1.25	0.70
		SD+LD	33	10	0.51	4.89	0.96	0.90	2.79	0.87	2.50	1.40	0.74
		SNV+SD	18	11	0.46	5.47	0.97	0.79	3.18	0.90	1.31	1.92	0.81
	Log(1/R)	None	4	3	1.21	2.06	0.76	1.39	1.79	0.70	1.77	1.25	0.60
		SNV	17	11	0.84	2.98	0.89	1.21	2.07	0.77	1.65	1.33	0.71
		SD	18	6	0.79	3.16	0.90	1.13	2.21	0.80	1.72	1.30	0.68
		SD+LD	15	3	1.10	2.27	0.81	1.28	1.95	0.74	1.34	1.66	0.76
		SNV+SD	13	8	0.55	4.51	0.95	0.70	3.56	0.92	1.38	1.86	0.80

SR	**R**	None	14	8	0.96	2.59	0.85	1.39	1.79	0.71	1.66	1.35	0.76
		SNV	1	1	1.78	1.40	0.49	1.86	1.34	0.44	2.21	1.31	0.60
		SD	7	4	1.01	2.47	0.84	1.27	1.96	0.74	1.64	1.35	0.67
		SD+LD	3	3	1.08	2.30	0.81	1.27	1.97	0.74	1.55	1.42	0.73
		SNV+SD	1	1	1.34	1.87	0.71	1.43	1.74	0.67	1.84	1.28	0.66
	Log(1/R)	None	11	8	0.95	2.64	0.86	1.29	1.94	0.74	1.44	1.59	0.75
		SNV	15	6	1.15	2.16	0.79	1.50	1.67	0.64	1.36	1.63	0.74
		SD	1	1	1.26	1.97	0.74	1.34	1.87	0.71	2.00	1.10	0.48
		SD+LD	5	3	1.09	2.28	0.81	1.26	1.98	0.75	1.96	1.23	0.56
		SNV+SD	7	5	1.00	2.48	0.84	1.30	1.92	0.73	1.95	1.64	0.76
EMCVS	**R**	None	6	3	1.05	1.94	0.73	1.18	1.72	0.67	2.07	1.10	0.57
		SNV	8	6	0.93	2.69	0.86	1.16	2.16	0.79	1.72	1.30	0.79
		SD	5	3	0.82	3.06	0.89	0.94	2.66	0.86	1.84	1.33	0.70
		SD+LD	10	5	0.74	3.38	0.91	0.89	2.81	0.87	2.11	1.25	0.68
		SNV+SD	7	3	0.90	2.77	0.87	1.02	2.44	0.83	1.52	1.47	0.72
	Log(1/R)	None	43	8	0.85	2.93	0.88	1.18	2.12	0.79	1.54	1.43	0.71
		SNV	9	3	1.02	2.45	0.83	1.13	2.20	0.79	1.64	1.44	0.71
		SD	10	7	0.69	3.63	0.92	0.89	2.82	0.87	1.42	1.58	0.73
		SD+LD	8	5	0.70	3.54	0.92	0.83	3.01	0.89	1.56	1.48	0.72
		SNV+SD	**6**	**5**	**0.88**	**2.83**	**0.88**	**1.03**	**2.42**	**0.83**	**1.17**	**1.88**	**0.83**

SR, selectivity ratio: VIP, variable importance projection: EMCVS, ensemble Monte Carlo variable selection; SD, second derivative; SNV, standard normal variate; LD, linear detrend; #Bands, wavelengths used for model development; #LVs, latent variables. The overall best model for 4 ºC is highlighted in bold.

Appendix 2. Performance of the TVC PLS-R models developed using VIS-SWNIR (445 - 970 nm) data from beef *LD* samples stored at 10 ºC. PLS full spectral range on reflectance (R) and logarithmic transformed (log(1/R)) spectral data is compared with spectral pre-treatments (SNV, SD, SD+LD, SNV+SD) and band selection methods (VIP, SR and EMCVS).

Chemometric method		Spectral Pre-treatment	# Bands	# LV	Calibration			Cross validation			Prediction		
					RMSEc	RPDc	R^2c	RMSEcv	RPDcv	R^2cv	RMSEp	RPDp	R^2p
PLS	R	None	106	8	0.37	5.84	0.97	0.64	3.38	0.92	1.38	1.66	0.75
		SNV	106	7	0.39	5.59	0.97	0.63	3.45	0.92	1.39	1.56	0.74
		SD	100	6	0.66	3.27	0.91	1.00	2.17	0.79	1.18	1.67	0.75
		SD+LD	100	5	0.69	3.13	0.90	1.02	2.12	0.78	1.15	1.72	0.76
		SNV+SD	100	4	0.60	3.59	0.92	0.81	2.68	0.86	0.80	2.63	0.89
	Log(1/R)	None	106	8	0.42	5.14	0.96	0.71	3.05	0.89	1.14	2.48	0.88
		SNV	106	7	0.42	5.13	0.96	0.69	3.15	0.90	1.02	2.32	0.86
		SD	100	4	0.64	3.41	0.91	0.84	2.58	0.85	1.21	1.84	0.80
		SD+LD	100	5	0.53	4.11	0.94	0.74	2.92	0.88	1.16	2.02	0.82
		SNV+SD	100	5	0.54	4.05	0.94	0.73	2.98	0.89	1.01	2.31	0.87
VIP	R	None	20	8	0.48	4.49	0.95	0.73	2.97	0.89	1.06	1.99	0.84
		SNV	37	8	0.41	5.29	0.96	0.63	3.42	0.91	1.58	1.27	0.72
		SD	33	5	0.76	2.86	0.88	1.03	2.10	0.78	1.09	1.77	0.81
		SD+LD	27	6	0.72	3.03	0.89	1.05	2.06	0.76	0.91	1.97	0.82
		SNV+SD	9	4	0.65	3.34	0.91	0.80	2.72	0.87	0.92	2.27	0.87
	Log(1/R)	None	15	6	0.52	4.13	0.94	0.72	3.03	0.89	1.10	2.42	0.88
		SNV	**33**	**7**	**0.53**	**4.11**	**0.94**	**0.79**	**2.75**	**0.87**	**0.83**	**3.10**	**0.93**
		SD	10	5	0.63	3.44	0.92	0.80	2.70	0.86	1.12	1.94	0.83
		SD+LD	13	4	0.66	3.29	0.91	0.80	2.71	0.86	1.34	1.59	0.78
		SNV+SD	10	5	0.60	3.59	0.92	0.78	2.78	0.87	1.04	2.16	0.87
SR	R	None	8	5	1.07	2.02	0.75	1.30	1.66	0.65	0.82	2.67	0.93

		SNV	21	9	0.55	3.97	0.94	0.87	2.50	0.84	0.95	2.20	0.86
		SD	13	6	0.67	3.25	0.91	0.92	2.35	0.82	1.00	2.07	0.87
		SD+LD	17	6	0.74	2.94	0.88	1.04	2.08	0.77	0.88	2.37	0.89
		SNV+SD	20	7	0.60	3.59	0.92	0.88	2.46	0.84	0.91	2.09	0.86
		None	8	5	0.90	2.39	0.83	1.12	1.93	0.73	1.07	2.12	0.86
		SNV	16	7	0.52	4.16	0.94	0.82	2.64	0.86	0.81	3.16	0.93
	Log(1/R)	SD	9	7	0.54	4.05	0.94	0.73	2.96	0.89	1.38	1.81	0.79
		SD+LD	17	4	0.67	3.25	0.91	0.85	2.55	0.85	1.34	1.64	0.79
		SNV+SD	17	4	0.65	3.32	0.91	0.86	2.51	0.84	1.15	1.98	0.85
		None	24	5	0.44	4.94	0.96	0.55	3.91	0.93	1.51	1.47	0.77
		SNV	18	4	0.45	4.85	0.96	0.56	3.85	0.93	1.73	1.19	0.73
	R	SD	13	3	0.75	2.90	0.88	0.87	2.49	0.84	1.00	1.78	0.80
		SD+LD	7	5	0.63	3.43	0.91	0.77	2.80	0.87	1.15	1.60	0.75
		SNV+SD	6	3	0.63	3.44	0.92	0.72	3.01	0.89	1.02	1.84	0.79
EMCVS		None	9	5	0.44	4.93	0.96	0.55	3.93	0.94	1.03	2.30	0.87
		SNV	7	6	0.48	4.51	0.95	0.65	3.34	0.91	1.00	2.40	0.88
	Log(1/R)	SD	10	3	0.66	3.29	0.91	0.75	2.89	0.88	1.04	1.96	0.83
		SD+LD	11	3	0.67	3.23	0.90	0.77	2.83	0.88	1.12	1.87	0.82
		SNV+SD	9	4	0.53	4.08	0.94	0.65	3.36	0.91	0.84	2.50	0.89

SR, selectivity ratio: VIP, variable importance projection: EMCVS, ensemble Monte Carlo variable selection; SD, second derivative; SNV, standard normal variate; LD, linear detrend; #Bands, wavelengths used for model development; #LVs, latent variables. The overall best model for 10 ºC is highlighted in bold.

Appendix 3. Performance of the TVC PLS-R models developed using VIS-SWNIR (445 - 970 nm) data from beef *LD* samples stored at 4 ºC or 10 ºC. PLS full spectral range on reflectance (R) and logarithmic transformed (log(1/R)) spectral data is compared with spectral pre-treatments (SNV, SD, SD+LD, SNV+SD) and band selection methods (VIP, SR and EMCVS).

Chemometric method	Spectral Pre-treatment	# Bands	# LV	Calibration			Cross validation			Prediction		
				RMSEc	RPDc	R^2c	RMSEcv	RPDcv	R^2cv	RMSEp	RPDp	R^2p
PLS	R	None	106	6	0.95	2.46	0.83	1.11	2.11	0.78	1.40	1.52	0.75
		SNV	106	6	0.85	2.76	0.87	1.01	2.32	0.81	1.33	1.47	0.78
		SD	100	5	0.96	2.43	0.83	1.19	1.96	0.74	1.11	1.76	0.79
		SNV+SD	100	7	0.86	2.72	0.87	1.09	2.15	0.78	0.98	1.99	0.84
		SD+LD	100	6	0.92	2.53	0.84	1.15	2.04	0.76	1.22	1.61	0.76
	Log(1/R)	None	106	6	0.92	2.54	0.85	1.17	2.00	0.76	1.23	1.71	0.77
		SNV	106	6	0.83	2.83	0.87	0.98	2.39	0.83	1.36	1.44	0.73
		SD	100	5	0.90	2.59	0.85	1.11	2.11	0.78	1.11	1.80	0.79
		SNV+SD	100	4	0.94	2.50	0.84	1.09	2.14	0.78	1.11	1.76	0.79
		SD+LD	100	4	0.94	2.49	0.84	1.13	2.07	0.77	1.16	1.71	0.77
VIP	R	None	8	5	1.03	2.28	0.81	1.13	2.06	0.77	1.51	1.42	0.69
		SNV	22	7	0.86	2.73	0.87	0.96	2.43	0.83	1.55	1.28	0.74
		SD	7	4	1.19	1.96	0.74	1.29	1.82	0.70	1.08	1.85	0.80
		SNV+SD	8	3	1.21	1.93	0.73	1.32	1.77	0.68	1.31	1.63	0.74
		SD+LD	19	6	1.12	2.09	0.77	1.26	1.85	0.71	1.32	1.51	0.72
	Log(1/R)	None	8	3	1.04	2.26	0.80	1.09	2.14	0.78	1.51	1.37	0.65
		SNV	10	6	0.92	2.55	0.85	1.03	2.28	0.81	1.24	1.68	0.77
		SD	30	4	0.99	2.37	0.82	1.12	2.08	0.77	1.15	1.76	0.78
		SNV+SD	24	5	0.95	2.46	0.83	1.10	2.12	0.78	1.06	1.88	0.80
		SD+LD	15	5	1.03	2.27	0.81	1.15	2.03	0.76	1.28	1.57	0.72
SR	R	None	7	5	1.41	1.66	0.64	1.59	1.47	0.54	1.44	1.60	0.74
		SNV	14	8	1.11	2.11	0.78	1.24	1.89	0.72	1.27	1.74	0.81

		SD	16	6	1.08	2.16	0.79	1.24	1.89	0.72	1.17	1.70	0.78
		SNV+SD	11	6	1.10	2.13	0.78	1.25	1.87	0.72	1.25	1.58	0.74
		SD+LD	17	6	1.02	2.29	0.81	1.20	1.96	0.74	1.24	1.60	0.75
		None	14	7	1.02	2.30	0.81	1.23	1.90	0.73	1.27	1.63	0.74
		SNV	17	5	1.02	2.29	0.81	1.22	1.92	0.73	1.24	1.61	0.75
	Log(1/R)	SD	13	7	0.97	2.40	0.83	1.15	2.03	0.76	1.23	1.70	0.76
		SNV+SD	17	5	1.07	2.18	0.79	1.24	1.89	0.72	1.41	1.43	0.68
		SD+LD	14	6	0.99	2.37	0.82	1.16	2.02	0.76	1.11	1.81	0.79
		None	3	2	1.02	1.65	0.63	1.07	1.57	0.59	1.66	1.29	0.60
		SNV	9	6	0.81	2.90	0.88	0.90	2.61	0.85	1.56	1.27	0.74
	R	SD	3	3	1.10	2.13	0.78	1.17	2.01	0.75	1.01	1.97	0.83
		SNV+SD	**8**	**4**	**0.94**	**2.48**	**0.84**	**1.05**	**2.22**	**0.80**	**0.95**	**2.10**	**0.85**
		SD+LD	4	3	0.92	2.55	0.85	0.96	2.43	0.83	1.24	1.61	0.76
EMCVS		None	23	13	0.61	3.82	0.93	0.77	3.04	0.89	0.88	2.25	0.86
		SNV	15	6	0.91	2.57	0.85	1.01	2.32	0.81	1.20	1.71	0.78
	Log(1/R)	SD	8	6	0.93	2.50	0.84	1.05	2.22	0.80	1.21	1.69	0.76
		SNV+SD	8	3	0.95	2.45	0.83	1.01	2.31	0.81	0.96	2.10	0.84
		SD+LD	9	3	0.95	2.45	0.83	1.03	2.27	0.81	1.04	1.92	0.81

SR, selectivity ratio: VIP, variable importance projection: EMCVS, ensemble Monte Carlo variable selection; SD, second derivative; SNV, standard normal variate; LD, linear detrend; #Bands, wavelengths used for model development; #LVs, latent variables. The overall best model for 10 ºC is highlighted in bold.

Appendix 4. Performance of the TVC PLS-R models developed using NIR (957 - 1664 nm) data from beef *LD* samples stored at 4 ºC, PLS full spectral range on reflectance (R) and logarithmic transformed (log(1/R)) spectral data is compared with spectral pre-treatments (SNV, SD, SD+LD, SNV+SD) and band selection methods (VIP, SR and EMCVS).

Chemometric method		Spectral Pre-treatment	# Bands	# LV	Calibration			Cross validation			Prediction		
					RMSEc	RPDc	R^2c	RMSEcv	RPDcv	R^2cv	RMSEp	RPDp	R^2p
PLS	R	None	102	8	0.66	3.58	0.92	1.14	2.07	0.78	2.75	0.94	0.45
		SD	96	5	0.84	2.79	0.87	1.17	2.00	0.75	1.97	1.68	0.84
		SD+LD	96	5	0.84	2.79	0.87	1.15	2.04	0.76	1.91	1.72	0.84
		SNV+SD	96	5	0.87	2.70	0.86	1.19	1.97	0.74	1.66	1.69	0.83
	Log(1/R)	None	102	6	0.82	2.87	0.88	1.21	1.94	0.75	3.50	0.69	0.08
		SD	96	5	0.92	2.55	0.85	1.45	1.62	0.63	0.87	2.23	0.91
		SD+LD	96	5	0.93	2.52	0.84	1.43	1.64	0.64	0.83	2.33	0.91
		SNV+SD	96	4	0.72	3.28	0.91	0.97	2.42	0.83	1.19	1.63	0.82
VIP	R	None	12	7	0.66	3.55	0.92	1.03	2.28	0.82	2.89	1.33	0.61
		SD	17	5	0.85	2.76	0.87	1.14	2.06	0.77	2.74	1.23	0.57
		SD+LD	17	5	0.93	2.52	0.84	1.20	1.95	0.74	1.91	1.59	0.72
		SNV+SD	12	7	0.83	2.82	0.87	1.08	2.17	0.79	1.94	1.45	0.68
	Log(1/R)	None	14	7	0.60	3.93	0.94	0.86	2.72	0.87	2.88	0.96	0.27
		SD	11	6	0.86	2.72	0.86	1.11	2.11	0.78	1.58	2.25	0.86
		SD+LD	8	6	0.88	2.68	0.86	1.08	2.17	0.79	1.22	2.07	0.86
		SNV+SD	7	4	0.76	3.07	0.89	0.94	2.50	0.84	1.24	1.87	0.80
SR	R	None	42	6	1.02	2.29	0.81	1.32	1.78	0.69	1.57	1.78	0.86
		SD	4	3	1.21	1.94	0.73	1.38	1.70	0.66	1.22	1.91	0.82
		SD+LD	2	1	1.57	1.49	0.55	1.64	1.43	0.51	1.73	1.37	0.64
		SNV+SD	1	1	1.51	1.55	0.58	1.59	1.48	0.54	2.28	1.01	0.32
	Log(1/R)	None	29	6	1.04	2.26	0.80	1.40	1.68	0.66	1.12	2.26	0.87
		SD	6	2	1.44	1.63	0.62	1.58	1.49	0.55	1.23	2.00	0.90

		SD+LD	4	4	1.35	1.74	0.67	1.60	1.47	0.54	1.13	2.12	0.91
		SNV+SD	1	1	1.67	1.40	0.49	1.75	1.34	0.44	2.56	0.90	0.15
EMCVS	**R**	None	8	5	0.72	3.24	0.90	1.00	2.34	0.82	3.91	0.82	0.07
		SD	16	4	0.94	2.50	0.84	1.14	2.06	0.76	2.83	1.30	0.63
		SD+LD	6	4	0.93	2.52	0.84	1.10	2.14	0.78	1.98	1.59	0.73
		SNV+SD	8	6	0.65	3.63	0.92	0.79	2.95	0.89	1.15	2.18	0.85
	Log(1/R)	None	19	5	0.86	2.69	0.86	1.06	2.20	0.79	3.85	0.75	0.01
		SD	10	4	0.80	2.93	0.88	1.01	2.32	0.82	0.93	2.48	0.89
		SD+LD	**13**	**4**	**0.78**	**3.03**	**0.89**	**1.01**	**2.31**	**0.81**	**0.92**	**3.00**	**0.92**
		SNV+SD	5	4	0.73	3.22	0.90	0.88	2.68	0.86	1.51	1.54	0.70

SR, selectivity ratio: VIP, variable importance projection: EMCVS, ensemble Monte Carlo variable selection; SD, second derivative; SNV, standard normal variate; LD, linear detrend; #Bands, wavelengths used for model development; #LVs, latent variables. The overall best model for 4 ºC is highlighted in bold.

Appendix 5. Performance of the TVC PLS-R models developed using NIR (957 - 1664 nm) data from beef *LD* samples stored at 10 ºC, PLS full spectral range on reflectance (R) and logarithmic transformed (log(1/R)) spectral data is compared with spectral pre-treatments (SNV, SD, SD+LD, SNV+SD) and band selection methods (VIP, SR and EMCVS).

Chemometric method		Pre-treatment	# Bands	# LV	Calibration			Cross validation			Prediction		
					RMSEc	RPDc	R^2c	RMSEcv	RPDcv	R^2cv	RMSEp	RPDp	R^2p
PLS	R	None	102	11	0.59	3.68	0.93	1.06	2.04	0.77	1.90	1.16	0.62
		SNV	102	5	1.03	2.10	0.77	1.39	1.55	0.60	2.19	1.23	0.54
		SD	96	7	0.71	3.07	0.89	1.21	1.79	0.70	2.05	0.98	0.47
		SD+LD	96	4	1.27	1.71	0.66	1.52	1.43	0.51	1.67	1.28	0.55
		SNV+SD	96	6	0.73	2.97	0.89	1.07	2.02	0.76	1.59	1.31	0.63
	Log(1/R)	None	102	11	0.55	3.91	0.93	1.07	2.02	0.76	2.38	0.80	0.35
		SNV	102	12	0.41	5.29	0.96	0.90	2.41	0.83	1.67	1.53	0.73
		SD	96	7	0.68	3.18	0.90	1.11	1.95	0.74	1.38	1.33	0.64
		SD+LD	96	6	0.79	2.75	0.87	1.29	1.68	0.65	1.37	1.31	0.63
		SNV+SD	96	7	0.61	3.56	0.92	1.03	2.12	0.78	1.19	1.57	0.72
EMCVS	R	None	19	9	0.68	3.19	0.90	1.00	2.17	0.79	1.79	1.02	0.51
		SNV	4	4	1.00	2.10	0.77	1.17	1.79	0.69	1.93	1.05	0.41
		SD	8	4	0.90	2.40	0.83	1.04	2.08	0.77	1.59	1.34	0.64
		SD+LD	7	4	0.81	2.67	0.86	0.96	2.26	0.81	1.37	1.31	0.65
		SNV+SD	14	3	0.80	2.72	0.86	0.90	2.39	0.83	1.64	1.43	0.69
	Log(1/R)	None	12	8	0.63	3.46	0.92	0.88	2.45	0.84	2.57	0.70	0.31
		SNV	**19**	**9**	**0.44**	**4.93**	**0.96**	**0.67**	**3.22**	**0.90**	**1.15**	**2.23**	**0.87**
		SD	12	5	0.78	2.78	0.87	0.96	2.25	0.80	1.71	1.35	0.67
		SD+LD	9	4	1.03	2.11	0.78	1.14	1.91	0.73	1.49	1.15	0.51
		SNV+SD	15	5	0.71	3.05	0.89	0.92	2.36	0.82	1.45	1.30	0.60
SR	R	None	1	1	2.14	1.01	0.03	2.32	0.93	0.12	1.93	0.90	0.29
		SNV	7	5	1.28	1.69	0.65	1.58	1.37	0.49	2.22	0.84	0.26

		SD	2	1	1.45	1.49	0.55	1.55	1.40	0.49	1.80	0.96	0.30
		SD+LD	1	1	1.72	1.26	0.37	1.84	1.18	0.29	2.26	0.77	0.12
		SNV+SD	1	1	1.91	1.14	0.23	2.03	1.07	0.14	1.90	1.04	0.36
		None	1	1	2.14	1.01	0.02	2.32	0.93	0.15	1.95	0.89	0.26
		SNV	1	1	1.92	1.13	0.21	2.04	1.06	0.13	1.50	1.23	0.72
	Log(1/R)	SD	1	1	1.91	1.13	0.22	2.00	1.08	0.15	1.74	0.99	0.29
		SD+LD	1	1	1.91	1.14	0.23	2.00	1.09	0.16	1.73	1.00	0.30
		SNV+SD	4	3	1.49	1.46	0.53	1.78	1.22	0.36	1.82	1.07	0.39
		None	6	4	1.32	1.64	0.63	1.55	1.40	0.49	2.17	0.89	0.28
		SNV	21	8	0.74	2.92	0.88	1.14	1.90	0.74	1.95	1.30	0.60
	R	SD	6	4	1.07	2.02	0.76	1.22	1.78	0.69	1.47	1.64	0.76
		SD+LD	5	3	1.40	1.55	0.58	1.59	1.36	0.47	1.91	1.14	0.54
		SNV+SD	9	4	0.87	2.48	0.84	1.03	2.10	0.77	1.82	1.71	0.77
VIP		None	13	9	0.82	2.65	0.86	1.18	1.84	0.71	1.78	1.79	0.86
		SNV	20	10	0.54	4.00	0.94	1.04	2.07	0.78	1.82	1.12	0.53
	Log(1/R)	SD	24	8	0.67	3.23	0.90	0.98	2.22	0.80	1.40	1.35	0.66
		SD+LD	22	6	0.90	2.42	0.83	1.18	1.84	0.70	1.61	1.15	0.54
		SNV+SD	31	8	0.67	3.23	0.90	0.98	2.21	0.80	1.14	1.65	0.75

SR, selectivity ratio: VIP, variable importance projection: EMCVS, ensemble Monte Carlo variable selection; SD, second derivative; SNV, standard normal variate; LD, linear detrend; #Bands, wavelengths used for model development; #LVs, latent variables. The overall best model for 10 ºC is highlighted in bold.

Appendix 6. Performance of the TVC PLS-R models developed using NIR (957 - 1664 nm) data from beef *LD* samples stored either 4 ºC or 10 ºC. PLS full spectral range on reflectance (R) and logarithmic transformed (log(1/R)) spectral data is compared with spectral pre-treatments (SNV, SD, SD+LD, SNV+SD) and band selection methods (VIP, SR and EMCVS).

Chemometric method		Spectral Pre-treatment	# Bands	# LV	Calibration			Cross validation			Prediction		
					RMSEc	RPDc	R^2c	RMSEcv	RPDcv	R^2cv	RMSEp	RPDp	R^2p
PLS	R	None	102	6	1.36	1.72	0.66	1.57	1.49	0.55	2.19	0.89	0.29
		SNV	102	13	0.86	2.72	0.86	1.27	1.85	0.71	2.58	1.00	0.44
		SD	96	6	1.19	1.97	0.74	1.40	1.67	0.64	1.27	1.53	0.71
		SNV+SD	96	7	1.06	2.20	0.79	1.36	1.72	0.67	1.58	1.25	0.61
		SD+LD	96	6	1.20	1.94	0.73	1.42	1.65	0.64	1.29	1.52	0.71
	Log(1/R)	None	102	5	1.51	1.55	0.58	1.74	1.34	0.45	2.78	0.72	0.14
		SNV	102	13	0.84	2.79	0.87	1.38	1.70	0.67	1.44	1.35	0.64
		SD	96	6	1.18	1.98	0.74	1.47	1.59	0.61	1.21	1.62	0.74
		SNV+SD	96	6	1.15	2.03	0.76	1.48	1.58	0.61	1.29	1.51	0.70
		SD+LD	96	6	1.17	2.01	0.75	1.47	1.59	0.61	1.18	1.66	0.76
VIP	R	None	9	5	1.41	1.65	0.63	1.56	1.50	0.56	2.52	0.79	0.22
		SNV	20	13	0.92	2.53	0.84	1.19	1.97	0.75	1.45	1.42	0.68
		SD	27	6	1.18	1.99	0.75	1.37	1.70	0.66	1.41	1.40	0.65
		SNV+SD	17	6	1.17	2.01	0.75	1.35	1.73	0.67	1.41	1.41	0.65
		SD+LD	6	4	1.36	1.72	0.66	1.47	1.59	0.60	1.34	1.46	0.67
	Log(1/R)	None	32	10	1.24	1.89	0.72	1.52	1.54	0.59	2.33	0.84	0.27
		SNV	10	5	1.35	1.73	0.67	1.52	1.53	0.58	1.93	1.09	0.44
		SD	17	6	1.23	1.90	0.72	1.41	1.66	0.64	1.29	1.58	0.72
		SNV+SD	12	6	1.21	1.93	0.73	1.40	1.67	0.65	1.17	1.66	0.75
		SD+LD	17	6	1.27	1.83	0.70	1.43	1.63	0.63	1.30	1.51	0.70
SR	R	None	28	7	1.40	1.67	0.64	1.93	1.21	0.41	1.31	1.49	0.70
		SNV	1	1	1.92	1.22	0.33	1.98	1.18	0.28	2.19	0.89	0.13

		SD	1	1	1.77	1.32	0.43	1.81	1.29	0.40	1.88	1.05	0.39
		SNV+SD	5	4	1.49	1.57	0.59	1.62	1.44	0.52	1.58	1.24	0.55
		SD+LD	1	1	1.72	1.36	0.46	1.77	1.32	0.43	1.93	1.02	0.37
		None	27	7	1.44	1.63	0.62	1.84	1.27	0.42	1.48	1.33	0.63
		SNV	11	3	1.91	1.23	0.34	2.07	1.13	0.23	2.32	0.86	0.11
	Log(1/R)	SD	1	1	1.94	1.20	0.31	1.98	1.18	0.28	1.84	1.13	0.45
		SNV+SD	1	1	2.10	1.12	0.20	2.16	1.08	0.15	2.14	0.92	0.18
		SD+LD	1	1	1.93	1.21	0.32	1.97	1.19	0.29	1.83	1.14	0.46
EMCVS		None	6	4	1.42	1.65	0.63	1.55	1.52	0.57	2.12	1.00	0.37
		SNV	19	11	0.85	2.76	0.87	1.09	2.15	0.79	1.77	1.23	0.56
	R	SD	10	4	1.31	1.78	0.69	1.42	1.65	0.63	1.48	1.45	0.67
		SNV+SD	12	5	1.04	2.24	0.80	1.18	1.98	0.74	1.15	1.75	0.77
		SD+LD	11	4	1.32	1.77	0.68	1.43	1.63	0.63	1.55	1.28	0.59
		None	12	6	1.36	1.70	0.65	1.55	1.49	0.55	2.08	0.95	0.32
		SNV	**19**	**11**	**0.90**	**2.60**	**0.85**	**1.14**	**2.05**	**0.77**	**1.03**	**1.92**	**0.81**
	Log(1/R)	SD	5	4	1.29	1.81	0.70	1.41	1.66	0.64	1.46	1.35	0.63
		SNV+SD	5	3	1.17	1.96	0.74	1.28	1.80	0.69	1.63	1.20	0.53
		SD+LD	6	4	1.25	1.87	0.72	1.37	1.71	0.66	1.48	1.35	0.64

Appendix 7. Performance of the best TVC PLS-R models developed using the LL data fusion of VIS-SWNIR (445 - 970 nm) and NIR (957 - 1664 nm) HSI data from beef LD samples stored at 4 ºC. PLS full spectral range on reflectance (R) and logarithmic transformed (log(1/R)) spectral data is compared with spectral pre-treatments (SNV, SD, SD+LD, SNV+SD) and band selection methods (VIP, SR and EMCVS).

Chemometric method	Spectral	Pre-treatment	# Bands	# LV	Calibration RMSEcv	Calibration RPDc	Calibration R^2c	Cross validation RMSEcv	Cross validation RPDcv	Cross validation R^2cv	Prediction RMSEp	Prediction RPDp	Prediction R^2p
PLS	R	None	208	7	0.87	2.85	0.88	1.53	1.63	0.66	1.73	1.23	0.68
		SNV	208	7	0.81	3.06	0.89	1.34	1.86	0.73	1.69	1.30	0.67
		SD	202	6	0.84	2.97	0.89	1.35	1.86	0.71	1.18	1.75	0.86
		SD+LD	202	6	0.85	2.94	0.88	1.38	1.81	0.70	1.17	1.76	0.86
		SNV+SD	202	6	0.82	3.05	0.89	1.15	2.17	0.79	1.35	1.52	0.77
	Log(1/R)	None	198	6	0.75	3.30	0.91	1.45	1.74	0.67	1.42	1.51	0.78
		SNV	208	6	0.75	3.32	0.91	1.06	2.35	0.82	1.36	1.57	0.75
		SD	208	7	0.71	3.49	0.92	1.11	2.25	0.80	1.32	1.66	0.78
		SD+LD	208	9	0.71	3.51	0.92	1.28	1.95	0.75	1.38	1.86	0.85
		SNV+SD	202	6	0.72	3.44	0.92	1.17	2.13	0.78	1.25	1.66	0.83
VIP	R	None	4	3	1.11	2.25	0.80	1.23	2.03	0.76	1.62	1.45	0.71
		SNV	24	5	0.97	2.56	0.85	1.26	1.97	0.74	1.74	1.27	0.63
		SD	22	11	0.56	4.42	0.95	1.11	2.27	0.81	1.74	1.65	0.83
		SD+LD	**22**	**8**	**0.76**	**3.28**	**0.91**	**1.09**	**2.30**	**0.81**	**1.16**	**1.90**	**0.88**
		SNV+SD	32	6	0.90	2.78	0.87	1.23	2.03	0.76	1.22	1.87	0.82
	Log(1/R)	None	10	7	0.88	2.82	0.87	1.31	1.91	0.75	1.48	1.52	0.72
		SNV	18	12	0.52	4.82	0.96	0.97	2.56	0.87	1.51	1.45	0.75
		SD	35	9	0.57	4.35	0.95	1.00	2.50	0.84	1.45	1.56	0.75
		SD+LD	29	12	0.50	4.99	0.96	0.95	2.64	0.86	1.58	1.61	0.74
		SNV+SD	10	7	0.86	2.90	0.88	1.32	1.90	0.72	1.34	1.71	0.77
SR	R	None	15	7	1.07	2.34	0.82	1.56	1.60	0.66	1.53	1.62	0.79

		SNV	17	9	0.92	2.72	0.87	1.36	1.83	0.71	1.00	2.22	0.87
		SD	8	4	1.00	2.49	0.84	1.27	1.96	0.74	1.60	1.37	0.68
		SD+LD	8	3	1.11	2.25	0.80	1.29	1.94	0.73	1.72	1.28	0.66
		SNV+SD	2	1	1.35	1.85	0.71	1.45	1.72	0.66	1.77	1.29	0.66
		None	15	8	0.91	2.73	0.87	1.39	1.80	0.73	1.52	1.48	0.74
		SNV	21	6	1.14	2.19	0.79	1.58	1.59	0.62	1.41	1.58	0.77
	Log(1/R)	SD	7	6	0.85	2.94	0.88	1.09	2.29	0.81	2.64	1.35	0.64
		SD+LD	1	1	1.24	2.01	0.75	1.31	1.90	0.72	2.08	1.05	0.44
		SNV+SD	8	5	0.91	2.72	0.87	1.13	2.21	0.80	1.97	1.78	0.83
		None	9	7	0.97	2.58	0.85	1.28	1.95	0.75	1.33	1.66	0.76
		SNV	5	4	1.02	2.32	0.81	1.15	2.06	0.76	1.74	1.29	0.58
	R	SD	9	6	0.71	3.51	0.92	0.91	2.74	0.87	1.71	1.29	0.81
		SD+LD	10	6	0.74	3.36	0.91	0.94	2.64	0.86	1.69	1.36	0.76
		SNV+SD	28	4	0.92	2.72	0.86	1.08	2.30	0.81	1.28	1.81	0.82
EMCVS		None	25	11	0.53	4.73	0.96	0.93	2.68	0.87	3.12	1.30	0.60
		SNV	11	4	0.70	3.54	0.92	0.94	2.66	0.86	1.94	1.34	0.61
	Log(1/R)	SD	6	4	0.77	3.22	0.90	0.92	2.72	0.87	1.54	1.43	0.68
		SD+LD	5	4	0.85	2.93	0.88	0.98	2.54	0.85	1.33	1.66	0.80
		SNV+SD	8	5	0.75	3.32	0.91	0.92	2.72	0.87	1.30	1.71	0.77

SR, selectivity ratio: VIP, variable importance projection: EMCVS, ensemble Monte Carlo variable selection; SD, second derivative; SNV, standard normal variate; LD, linear detrend; #Bands, wavelengths used for model development; #LVs, latent variables. The overall best model for the LL data fusion of 4 ºC data is highlighted in bold.

Appendix 8. Performance of the best TVC PLS-R models developed using the LL data fusion of VIS-SWNIR (445 - 970 nm) and NIR (957 - 1664 nm) HSI data from beef LD samples stored at 10 ºC. PLS full spectral range on reflectance (R) and logarithmic transformed (log(1/R)) spectral data is compared with spectral pre-treatments (SNV, SD, SD+LD, SNV+SD) and band selection methods (VIP, SR and EMCVS).

Chemometric method		Spectral Pre-treatment	# Bands	# LV	Calibration			Cross validation			Prediction		
					RMSEcv	RPDc	R^2c	RMSEcv	RPDcv	R^2cv	RMSEp	RPDp	R^2p
PLS	R	None	208	8	0.43	5.04	0.96	0.76	2.87	0.88	1.39	1.61	0.73
		SNV	208	7	0.42	5.20	0.96	0.67	3.25	0.91	1.41	1.87	0.79
		SD	202	7	0.58	3.72	0.93	0.95	2.28	0.81	1.11	1.86	0.79
		SD+LD	202	7	0.58	3.73	0.93	0.95	2.29	0.81	1.10	1.87	0.79
		SNV+SD	202	4	0.70	3.08	0.89	0.93	2.32	0.82	0.88	2.46	0.89
	Log(1/R)	None	208	8	0.44	4.90	0.96	0.77	2.82	0.88	1.64	1.59	0.76
		SNV	208	6	0.55	3.95	0.94	0.83	2.61	0.85	1.33	1.97	0.81
		SD	202	6	0.54	4.02	0.94	0.84	2.59	0.85	1.41	1.75	0.79
		SD+LD	202	6	0.54	4.05	0.94	0.83	2.61	0.85	1.39	1.78	0.80
		SNV+SD	202	6	0.48	4.49	0.95	0.76	2.85	0.88	1.23	1.97	0.83
EMCVS	R	None	20	6	0.43	5.09	0.96	0.59	3.68	0.93	1.26	1.89	0.81
		SNV	128	6	0.42	5.11	0.96	0.61	3.54	0.92	1.30	1.92	0.82
		SD	9	6	0.52	4.16	0.94	0.65	3.36	0.91	0.86	2.09	0.84
		SD+LD	10	7	0.49	4.45	0.95	0.64	3.40	0.91	0.97	1.98	0.84
		SNV+SD	12	5	0.49	4.39	0.95	0.68	3.17	0.90	1.20	1.76	0.77
		None	**11**	**6**	**0.46**	**4.66**	**0.95**	**0.58**	**3.71**	**0.93**	**0.94**	**3.03**	**0.94**
	Log(1/R)	SNV	7	5	0.59	3.69	0.93	0.75	2.90	0.88	1.13	2.22	0.86
		SD	7	3	0.62	3.49	0.92	0.71	3.04	0.89	0.98	2.05	0.84
		SD+LD	20	3	0.63	3.41	0.91	0.73	2.96	0.89	1.11	1.87	0.82
		SNV+SD	9	4	0.55	3.94	0.94	0.66	3.30	0.91	1.03	2.12	0.85
SR	R	None	8	5	1.07	2.02	0.75	1.30	1.66	0.65	0.82	2.67	0.93
		SNV	20	8	0.65	3.32	0.91	0.98	2.21	0.80	0.89	2.56	0.91

		SD	13	6	0.67	3.25	0.91	0.92	2.35	0.82	1.00	2.07	0.87
		SD+LD	23	7	0.74	2.93	0.88	1.08	2.01	0.75	0.74	2.51	0.90
		SNV+SD	11	6	0.73	2.96	0.89	0.97	2.24	0.80	1.20	1.81	0.84
		None	8	5	0.90	2.39	0.83	1.12	1.93	0.73	1.07	2.12	0.86
		SNV	25	8	0.70	3.08	0.89	1.14	1.91	0.73	1.50	1.40	0.84
	Log(1/R)	SD	25	5	0.54	4.04	0.94	0.80	2.70	0.86	1.13	2.02	0.83
		SD+LD	10	8	0.53	4.11	0.94	0.80	2.71	0.86	1.20	1.86	0.80
		SNV+SD	24	5	0.55	3.95	0.94	0.77	2.82	0.87	1.02	2.20	0.86
		None	21	10	0.40	5.48	0.97	0.59	3.68	0.93	1.21	1.77	0.78
		SNV	27	5	0.48	4.48	0.95	0.68	3.20	0.90	1.04	2.15	0.86
	R	SD	20	8	0.60	3.62	0.92	0.88	2.47	0.84	1.21	1.72	0.77
		SD+LD	16	8	0.61	3.56	0.92	0.89	2.43	0.83	1.24	1.66	0.75
		SNV+SD	14	5	0.73	2.97	0.89	0.94	2.31	0.81	0.84	2.50	0.89
VIP		None	14	7	0.48	4.52	0.95	0.68	3.17	0.90	1.11	2.35	0.87
		SNV	7	5	0.61	3.57	0.92	0.75	2.88	0.88	1.10	2.42	0.88
	Log(1/R)	SD	10	5	0.63	3.44	0.92	0.80	2.70	0.86	1.12	1.94	0.83
		SD+LD	14	4	0.63	3.43	0.92	0.80	2.70	0.86	1.16	1.85	0.82
		SNV+SD	10	5	0.58	3.72	0.93	0.74	2.92	0.88	1.01	2.12	0.85

SR, selectivity ratio: VIP, variable importance projection: EMCVS, ensemble Monte Carlo variable selection; SD, second derivative; SNV, standard normal variate; LD, linear detrend; #Bands, wavelengths used for model development; #LVs, latent variables. The overall best model for the LLDF of 10 ºC data is highlighted in bold.

Appendix 9. Performance of the best TVC PLS-R models developed using the LL data fusion of VIS-SWNIR (445 - 970 nm) and NIR (957 - 1664 nm) HSI data from beef *LD* samples stored at either 4 ºC or 10 ºC. PLS full spectral range on reflectance (R) and logarithmic transformed (log(1/R)) spectral data is compared with spectral pre-treatments (SNV, SD, SD+LD, SNV+SD) and band selection methods (VIP, SR and EMCVS).

Regression Model		Pre-treatment	# Bands	# LV	Calibration			Cross validation			Prediction		
					RMSEc	RPDc	R^2c	RMSEcv	RPDcv	R^2cv	RMSEp	RPDp	R^2p
PLS	R	None	208	8	0.86	2.72	0.86	1.06	2.21	0.8	1.38	1.43	0.72
		SNV	208	7	0.79	2.95	0.89	1.01	2.32	0.82	1.42	1.38	0.70
		SD	202	6	0.96	2.45	0.83	1.20	1.95	0.74	0.95	2.08	0.85
		SD+LD	202	7	0.89	2.64	0.86	1.16	2.02	0.75	1.00	2.04	0.85
		SNV+SD	202	7	0.83	2.82	0.87	1.07	2.19	0.79	1.12	1.86	0.81
	Log(1/R)	None	208	8	0.83	2.81	0.87	1.12	2.09	0.78	1.44	1.36	0.66
		SNV	208	5	0.94	2.50	0.84	1.09	2.14	0.78	1.33	1.49	0.71
		SD	202	6	0.88	2.66	0.86	1.10	2.13	0.78	1.17	1.71	0.77
		SD+LD	202	6	0.89	2.63	0.86	1.11	2.11	0.78	1.15	1.76	0.78
		SNV+SD	202	5	0.93	2.52	0.84	1.14	2.06	0.76	1.18	1.75	0.78
VIP	R	None	30	8	0.96	2.44	0.83	1.09	2.15	0.78	1.48	1.43	0.69
		SNV	13	7	0.96	2.45	0.83	1.09	2.15	0.78	1.40	1.44	0.73
		SD	15	7	1.03	2.27	0.81	1.22	1.91	0.73	1.07	1.86	0.80
		SD+LD	11	6	1.02	2.30	0.81	1.18	1.98	0.75	1.15	1.73	0.79
		SNV+SD	29	10	0.82	2.84	0.88	1.10	2.13	0.78	1.09	1.83	0.81
	Log(1/R)	None	10	4	1.06	2.21	0.8	1.14	2.06	0.76	1.49	1.35	0.66
		SNV	22	6	0.92	2.55	0.85	1.04	2.24	0.8	1.31	1.53	0.73
		SD	6	4	1.10	2.12	0.78	1.19	1.97	0.74	1.18	1.74	0.77
		SD+LD	6	3	1.08	2.17	0.79	1.12	2.10	0.77	1.21	1.67	0.75
		SNV+SD	10	4	1.04	2.25	0.8	1.17	2.00	0.75	1.27	1.66	0.75
SR	R	None	7	5	1.41	1.66	0.64	1.59	1.47	0.54	1.44	1.60	0.74

		SNV	20	9	0.97	2.42	0.83	1.33	1.75	0.68	1.24	1.75	0.78
		SD	12	8	1.05	2.23	0.80	1.23	1.91	0.73	1.06	1.87	0.82
		SD+LD	24	6	1.07	2.19	0.79	1.23	1.90	0.72	1.24	1.61	0.75
		SNV+SD	11	6	1.13	2.06	0.76	1.32	1.78	0.69	1.33	1.50	0.71
		None	14	7	1.02	2.3	0.81	1.23	1.90	0.73	1.27	1.63	0.74
		SNV	18	8	1.09	2.15	0.78	1.31	1.79	0.69	1.19	1.96	0.82
	Log(1/R)	SD	13	7	0.97	2.4	0.83	1.15	2.03	0.76	1.23	1.70	0.76
		SD+LD	19	5	0.98	2.38	0.82	1.1	2.12	0.78	1.25	1.61	0.74
		SNV+SD	15	7	0.95	2.46	0.84	1.15	2.04	0.76	1.36	1.59	0.72
		None	15	5	0.93	2.51	0.84	1.07	2.18	0.79	1.32	1.63	0.77
		SNV	52	6	0.86	2.73	0.87	0.98	2.4	0.83	1.37	1.48	0.73
	R	SD	6	3	1.06	2.21	0.80	1.13	2.06	0.76	1.15	1.73	0.79
		SD+LD	**35**	**4**	**0.96**	**2.45**	**0.83**	**1.12**	**2.08**	**0.77**	**0.87**	**2.27**	**0.88**
		SNV+SD	15	4	0.90	2.61	0.85	0.99	2.36	0.82	1.03	2.10	0.85
EMCVS		None	7	5	0.97	2.40	0.83	1.06	2.21	0.8	1.58	1.37	0.65
		SNV	17	8	0.87	2.68	0.86	1.03	2.26	0.81	1.32	1.70	0.76
	Log(1/R)	SD	6	3	0.99	2.36	0.82	1.07	2.18	0.79	1.04	1.91	0.81
		SD+LD	5	5	0.93	2.51	0.84	1.01	2.31	0.81	0.98	2.09	0.84
		SNV+SD	3	2	1.04	2.18	0.79	1.08	2.10	0.77	1.24	1.60	0.73

SR, selectivity ratio: VIP, variable importance projection: EMCVS, ensemble Monte Carlo variable selection; SD, second derivative; SNV, standard normal variate; LD, linear detrend; #Bands, wavelengths used for model development; #LVs, latent variables. The overall best model for the LLDF of 4 and 10 ºC combine data is highlighted in bold.

Table 1. TVC of beef *LD* samples (log CFU/g) stored at 4 and 10 ºC. Average value ± standard deviation (n = 3). Superscripts show the statistical significance between samples obtained with Tukey-Kramer test at $\alpha = 0.05$.

Temperature	Time (hours)	Sample id. /TVC S1	S2	S3	S7	S8	S9
4 ºC	0	7.1±0.4^{a,c}	6.9±0.2^{a,c}	7.0±0.5^{a,b}	5.3±0.1^{a}	5.3±0.4^{a}	3.4±0.5^{a}
	24	7.1±0.3^{a,c}	6.9±0.4^{a,c}	7.2±0.6^{a,b}	5.3±0.2^{a}	5.1±0.4^{a}	3.3±0.0^{a}
	96	8.9±0.1^{b,c,d,e}	8.6±0.2^{b,c,d,f,g}	8.3±0.3^{a,b,c}	6.6±0.4^{b}	7.1±0.7^{b}	4.1±0.3^{a}
	120	8.1±0.0^{a,b,c,e}	7.7±0.1^{a,b,c,d,g}	8.1±0.6^{a,b,c}	8.7±0.6^{c}	8.3±0.2^{c}	5.6±0.0^{b}
	192	8.8±0.4^{b,c,d,e}	9.1±0.2^{b,c,d,e,f,g}	8.4±0.3^{a,b,c}	9.4±0.1^{c}	9.4±0.2^{c}	7.7±0.5^{c,d}
	264	10.1±0.7^{b,d,e,f}	10.5±0.7^{d,e,f}	9.0±0.1^{b,c,d}	10.9±0.8^{d}	12.2±0.1^{d,e}	8.9±0.1^{c,d,e}
	288	9.5±0.3^{b,c,d,e,f}	9.7±0.6^{b,d,e,f,g,h}	10.2±0.3^{c,d,e}	12.2±0.3^{e,f}	12.1±0.3^{d,e,f}	9.2±0.2^{c,d,e}
	312	9.7±1.2^{b,c,d,e,f}	9.0±1.0^{b,c,d,f,g,h}	10.6±0.7^{d,e}	-	-	-
	336	-	-	-	13.2±0.2^{e,f,g}	13.5±0.7^{e,f}	10.5±1.3^{d,e}
	360	10.6±0.5^{d,e,f}	11.1±0.3^{f,h}	11.4±1.0^{d,e}	14.±0.3^{f,g}	14.1±0.1^{f,g}	-

Temperature	Time (hours)	Sample id. /TVC S4	S5	S6	S7	S8	S9
10 ºC	0	6.1±0.1^{a}	6.7±0.1^{a}	6.7±0.3^{a,b}	5.3±0.1^{a}	5.3±0.4^{a}	3.4±0.5^{a}
	12	6.7±0.3^{b,c}	7.7±0.2^{b}	6.9±0.1^{a,b}	-	-	-
	24	6.8±0.2^{b,c}	7.3±0.1^{b}	7.1±0.1^{a,b,c}	6.0±0.3^{a}	6.1±0.8^{a}	3.4±0.5^{a}
	36	6.9±4.0^{b,c,d}	7.7±0.1^{b}	7.1±0.2^{a,b,c}	-	-	-
	48	7.4±0.1^{c,d}	7.6±0.1^{b}	7.5±0.1^{b,c}	-	-	-
	84	9.2±0.1^{e,f,h}	9.4±0.1^{c,d,e,g}	9.3±0.2^{d,e}	-	-	-
	96	9.4±0.2^{e,f,h,i}	9.1±0.2^{c,d}	9.3±0.1^{d,e}	8.8±0.2^{b,c}	9.0±0.1^{b}	7.6±0.1^{b}
	108	9.9±0.1^{g,h,i}	9.8±0.2^{c,e,f,g}	9.6±0.1^{d,e,f}	-	-	-
	120	9.6±0.2^{e,f,g,h,i}	9.8±0.1^{c,e,f,g}	9.8±0.1^{e,f}	10.5±0.4^{b,c,d}	10.2±0.1^{c}	9.3±0.5^{c}
	132	10.1±0.2^{g,h,i}	10.0±0.1^{e,f,g}	9.9±0.1^{e,f}	-	-	-
	144	9.8±0.1^{f,g,h,i}	9.9±0.1^{c,e,f,g}	10.0±0.2^{e,f}	11.6±1.4^{c,d}	12.2±0.2^{d}	11.1±0.2^{d}
	168	-	-	-	12.3±0.0^{c,d}	13.1±0.1^{d}	12.3±0.3^{e}

Values followed by different letters in the same column are significantly different using ANOVA and Tukey test ($p < 0.05$).

Table 2. Performance of the best TVC PLS-R models developed for beef *LD* samples stored at 4 ºC using the full spectral range and optimum band selection method evaluated for VIS-SWNIR (445 - 970 nm) and NIR (957 - 1664 nm) HSI data.

Regression model		Pre-treatment		#	#	Calibration			Cross validation			Prediction		
		1st	2nd	Bands	LV	RMSEc	RPDc	R^2c	RMSEcv	RPDcv	R^2cv	RMSEp	RPDp	R^2p
445 - 970 nm														
PLS	R	SNV	SD	100	6	0.79	3.15	0.9	1.34	1.86	0.74	1.35	1.61	0.81
EMCVS	log(1/R)	SNV	SD	6	5	0.88	2.83	0.88	1.03	2.42	0.83	1.17	1.88	0.83
957 - 1664 nm														
PLS	log(1/R)	SD	AsLs	96	9	0.42	5.63	0.97	1.03	2.29	0.81	0.99	2.26	0.94
EMCVS	**log(1/R)**	**SD**	**AsLs**	**17**	**7**	**0.5**	**4.71**	**0.95**	**0.7**	**3.37**	**0.91**	**0.81**	**3.09**	**0.95**

EMCVS, ensemble Monte Carlo variable selection; SD, second derivative; SNV, standard normal variate; AsLs, asymmetric least squares; #Bands, wavelengths used for model development; #LVs, latent variables. The best overall model for 4 ºC is highlighted in bold.

Table 3. Performance of the best TVC PLS-R models developed for beef *LD* samples stored at 10 ºC using the full spectral range and optimum band selection method evaluated for VIS-SWNIR (445 - 970 nm) and NIR (957 - 1664 nm) HSI data.

Regression model		Pre-treatment		#	#	Calibration			Cross validation			Prediction		
		1st	2nd	Bands	LV	RMSEc	RPDc	R^2c	RMSEcv	RPDcv	R^2cv	RMSEp	RPDp	R^2p
445 - 970 nm														
PLS	R	SD	MS	100	6	0.48	4.52	0.95	0.7	3.08	0.89	1.09	2.84	0.92
EMCVS	**R**	**SD**	**MS**	**46**	**6**	**0.47**	**4.60**	**0.95**	**0.69**	**3.16**	**0.90**	**0.96**	**3.32**	**0.94**
957 - 1664 nm														
PLS	log(1/R)	SD	SNV	96	7	0.62	3.49	0.92	1.03	2.11	0.78	1.2	1.59	0.72
EMCVS	log(1/R)	SNV		19	9	0.44	4.93	0.96	0.67	3.22	0.90	1.15	2.23	0.87

EMCVS, ensemble Monte Carlo variable selection; MS, median scaled; SD, second derivative; SNV, standard normal variate; #Bands, wavelengths used for model development; #LVs, latent variables. The best overall model for 10 ºC is highlighted in bold.

Table 4. Performance of the best TVC PLS-R models developed for beef *LD* samples stored at either 4 ºC or 10 ºC using the full spectral range and optimum band selection method evaluated for VIS-SWNIR (445 - 970 nm) and NIR (957 - 1664 nm) HSI data.

Regression model		Pre-treatment		#	#	Calibration			Cross validation			Prediction		
		1st	2nd	Bands	LV	RMSEc	RPDc	R^2c	RMSEcv	RPDcv	R^2cv	RMSEp	RPDp	R^2p
445 - 970 nm														
PLS	R	SNV	SD	100	7	0.86	2.72	0.87	1.09	2.15	0.78	0.98	1.99	0.84
EMCVS	R	SNV	SD	8	4	0.94	2.48	0.84	1.05	2.22	0.80	0.95	2.10	0.85
957 - 1664 nm														
PLS	log(1/R)	SD	LD	202	4	1.17	2.01	0.75	1.47	1.59	0.61	1.18	1.66	0.76
EMCVS	R	SNV	SD	96	6	1.04	2.24	0.80	1.18	1.98	0.74	1.15	1.75	0.77

EMCVS, ensemble Monte Carlo variable selection; SNV, standard normal variate; LD, linear detrend; SD, second derivative; #Bands, wavelengths used for model development; #LVs, latent variables. The overall best model for the combined data of both temperatures is highlighted in bold.

Table 5. Performance of the best TVC PLS-R models developed using VIS-SWNIR (445 - 970 nm) and NIR (957 - 1664 nm) HSI data from beef *LD* samples stored at (i) 4 ºC, (ii) 10 ºC and (iii) either 4 ºC or 10 ºC using the optimum band selection method and LL, ML and HL data fusion

Regression model			Pre-treatment		#	#	Calibration			Cross validation			Prediction		
			1st	2nd	Bands	LV	RMSEc	RPDc	R^2c	RMSEcv	RPDcv	R^2cv	RMSEp	RPDp	R^2p
4 ºC															
VIS-SWNIR	EMCVS	log(1/R)	SNV	SD	6	5	0.88	2.83	0.88	1.03	2.42	0.83	1.17	1.88	0.83
NIR	EMCVS	log(1/R)	SD	AsLs	17	7	0.50	4.71	0.95	0.70	3.37	0.91	0.81	3.09	0.95
LL	VIP	R	SD	LD	22	8	0.76	3.28	0.91	1.09	2.30	0.81	1.16	1.90	0.88
ML						11	0.50	4.66	0.95	0.92	2.55	0.85	0.80	2.41	0.93
HL							**0.83**	**2.82**	**0.87**	**0.91**	**2.58**	**0.85**	**0.58**	**4.13**	**0.96**
10 ºC															
VIS-SWNIR	EMCVS	R	SD	MS	46	6	**0.47**	**4.60**	**0.95**	**0.69**	**3.16**	**0.90**	**0.96**	**3.32**	**0.94**
NIR	EMCVS	log(1/R)	SNV		19	9	0.44	4.93	0.96	0.67	3.22	0.90	1.15	2.23	0.87
LL	EMCVS	log(1/R)	None		11	6	0.46	4.66	0.95	0.58	3.71	0.93	0.94	3.03	0.94
ML						6	0.47	4.64	0.95	0.75	2.89	0.88	1.17	2.17	0.84
HL							**0.36**	**6.07**	**0.97**	**0.51**	**4.30**	**0.95**	**0.97**	**3.28**	**0.94**
4 ºC and 10 ºC															
VIS-SWNIR	EMCVS	R	SNV	SD	8	4	0.94	2.48	0.84	1.05	2.22	0.80	0.95	2.10	0.85
NIR	EMCVS	R	SNV	SD	96	6	1.04	2.24	0.80	1.18	1.98	0.74	1.15	1.75	0.77
LL	EMCVS	R	SD	LD	35	4	**0.96**	**2.45**	**0.83**	**1.12**	**2.08**	**0.77**	**0.87**	**2.27**	**0.88**
ML						5	0.79	2.96	0.89	0.93	2.51	0.84	1.32	1.49	0.74
HL							**0.84**	**2.79**	**0.88**	**0.94**	**2.47**	**0.84**	**0.89**	**2.27**	**0.86**

EMCVS, ensemble Monte Carlo variable selection; VIP, variable importance projection ; SD, second derivative; SNV, standard normal variate; AsLs, asymmetric least squares; LD, linear detrend; MS, medium scaled: #Bands, wavelengths used for model development; #LVs, latent variables. The best model for each storage temperature is highlighted in bold.

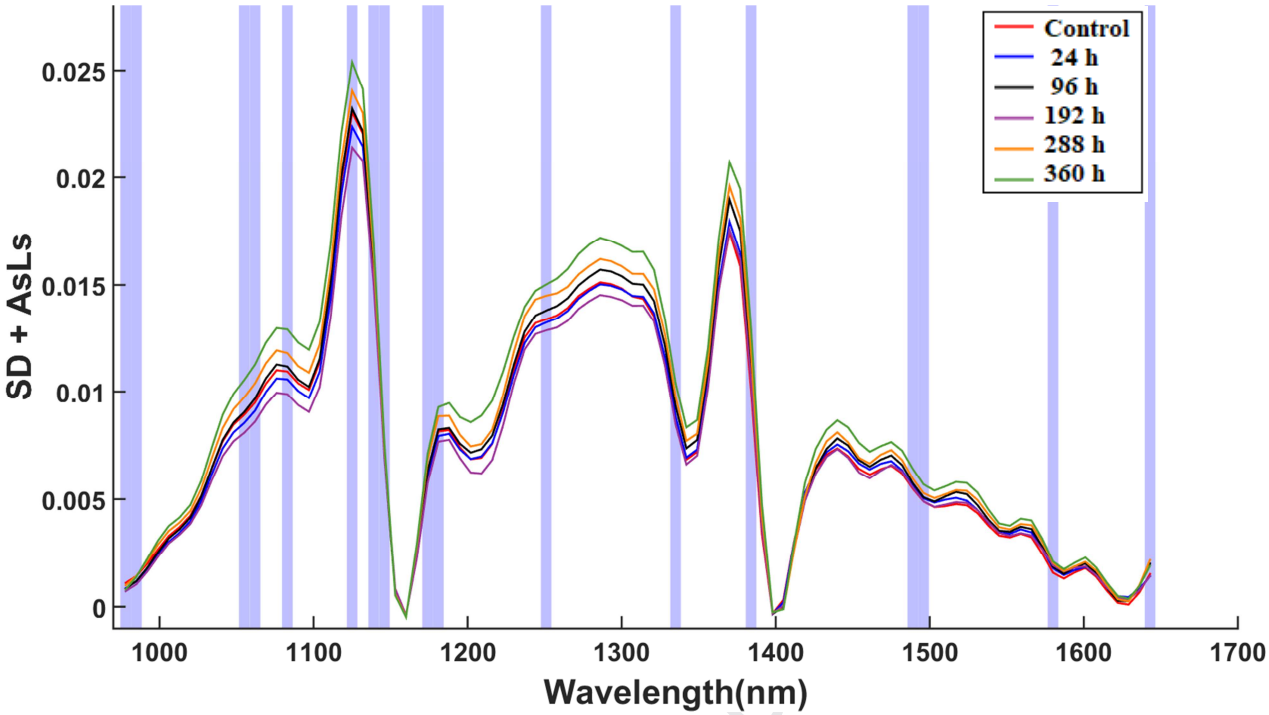

Fig. 1. Log (1/R) NIR pre-treated (SD+AsLs) spectra of beef *LD* samples stored at 4 ºC for selected storage times. Bands selected by the EMCVS method to predict TVC of samples are highlighted in blue.

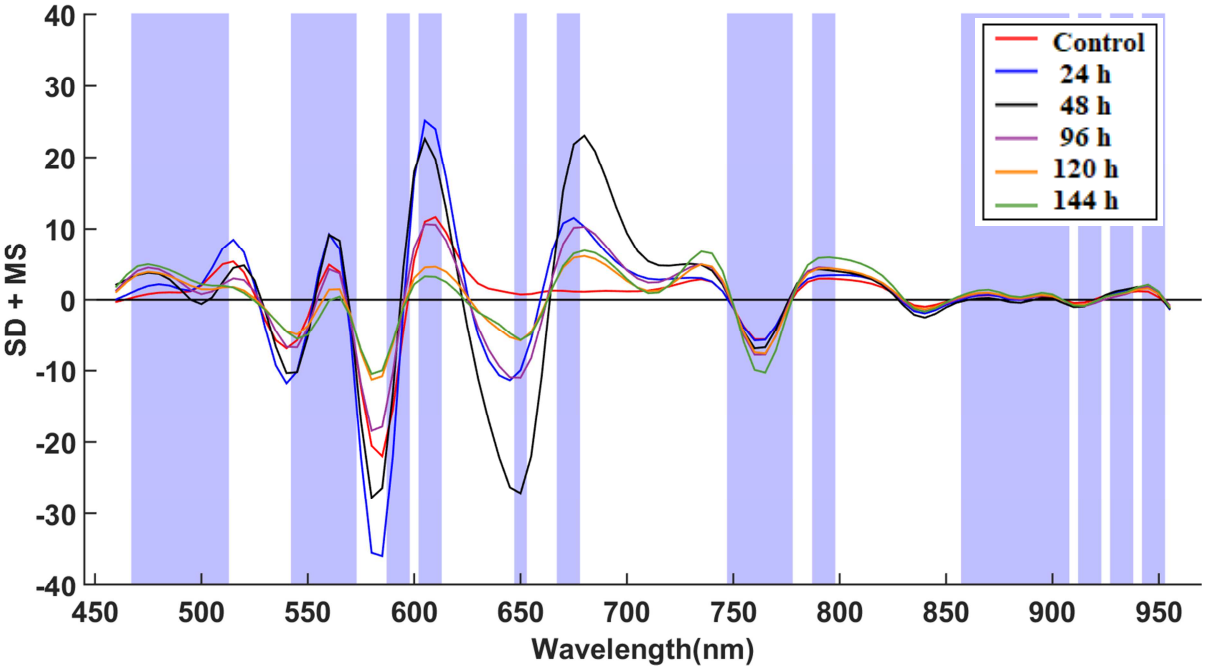

Fig. 2. Reflectance VIS-SWNIR pre-treated (SD+MS) spectra of beef *LD* samples stored at 10 ºC for selected storage times. Bands selected by the EMCVS method to predict TVC of samples are highlighted in blue.

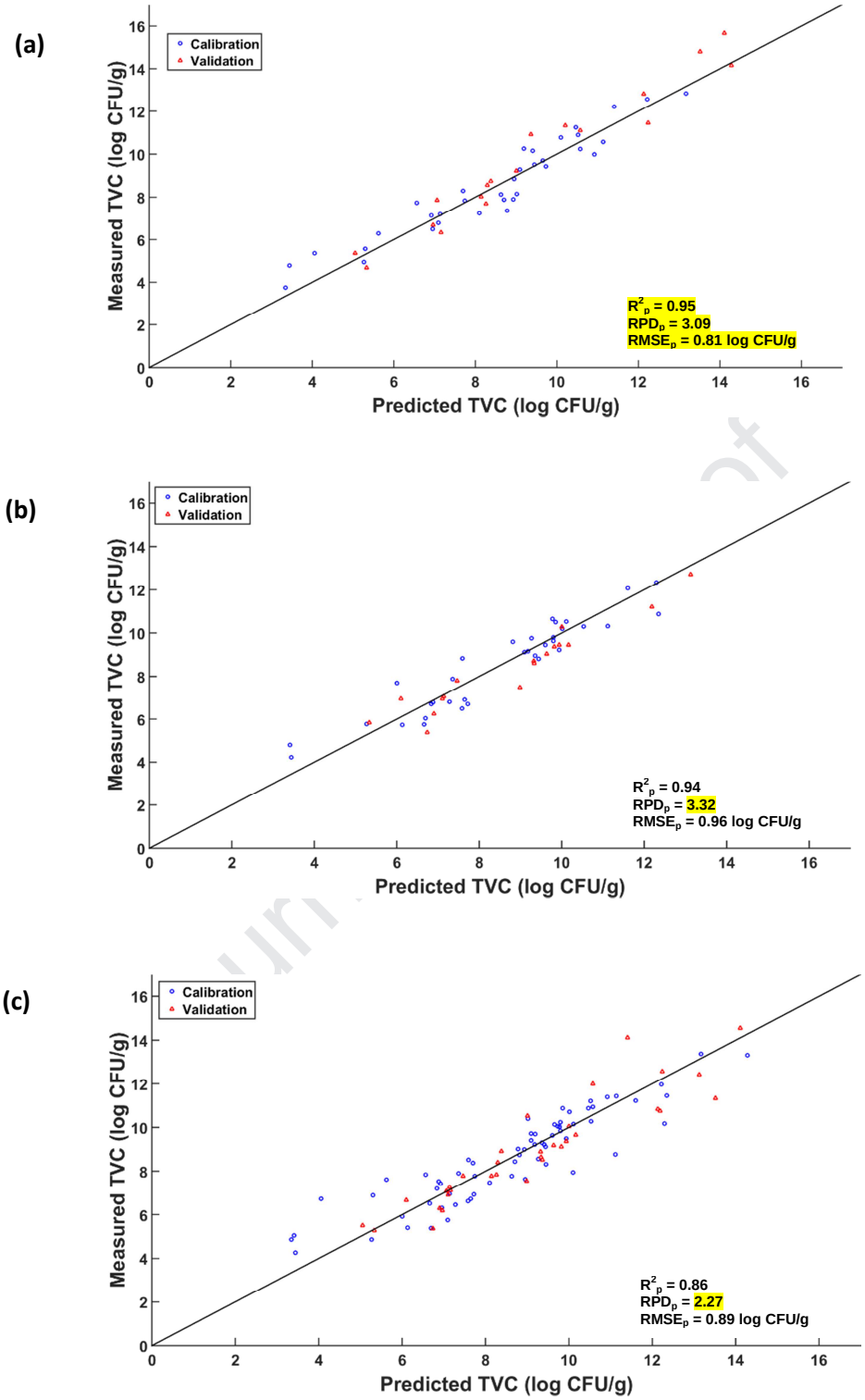

Fig. 3. Measured vs predicted TVC for the best performing PLS-R models developed for beef *LD* samples stored at (a) 4 ºC, (b) 10 ºC and (c) either 4 ºC or 10 ºC.

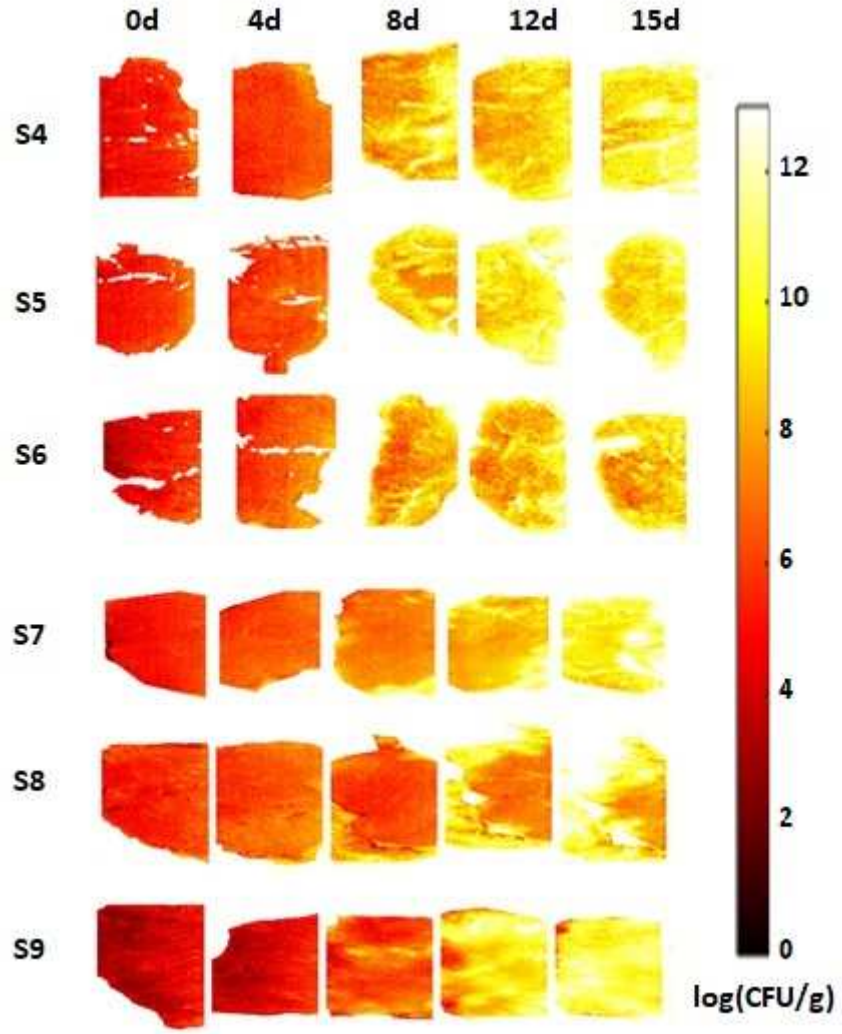

Fig. 4. Prediction maps for TVC of beef *LD* samples (log CFU/g) stored at 10 ºC for selected times using the reflectance VIS-SWNIR pre-treated (SD+MS) spectra which selected 46 bands).

- Microbial quality of beef stored under normal or abuse conditions can be predicted
- Spectral pre-treatments, band selection and data fusion methods are key for robust model development
- Hyperspectral imaging and chemometrics have potential for real-time monitoring of microbial quality

Conflict of Interest and Authorship Conformation Form

Please check the following as appropriate:

- ✓ All authors have participated in (a) conception and design, or analysis and interpretation of the data; (b) drafting the article or revising it critically for important intellectual content; and (c) approval of the final version.
- ✓ This manuscript has not been submitted to, nor is under review at, another journal or other publishing venue.
- ✓ The authors have no affiliation with any organization with a direct or indirect financial interest in the subject matter discussed in the manuscript
- o The following authors have affiliations with organizations with direct or indirect financial interest in the subject matter discussed in the manuscript:

Author's name	Affiliation